Construction and Building Materials 258 (2020) 119604

Contents lists available at ScienceDirect

Construction and Building Materials

journal homepage: www.elsevier.com/locate/conbuildmat

Evaluation of reactivity indexes and durability properties of slag-based geopolymer concrete incorporating corn cob ash

Solomon Oyebisi [a,*], Anthony Ede [a], Festus Olutoge [b], Samuel Ogbiye [a]

[a] Department of Civil Engineering, Covenant University, PMB. 1023, Ota, Nigeria
[b] Department of Civil and Environmental Engineering, University of the West Indies, St Augustine, Trinidad and Tobago

HIGHLIGHTS

- The activity indexes of GGBFS-CCA blends increase as CaO, MgO, and Al_2O_3 increase.
- Pozzolanic activity of GGBFS-CCA blends increases as SiO_2 and Al_2O_3 increase.
- AIs significantly correlate with the compressive strength of GGBFS-CCA GPC.
- GGBFS-CCA GPC offers a better resistance to sulfate attacks.

ARTICLE INFO

Article history:
Received 9 March 2020
Received in revised form 30 April 2020
Accepted 16 May 2020

Keywords:
Supplementary cementitious materials
Recycling
Waste management, geopolymer concrete
Mix design proportions
Sodium silicate
Sodium hydroxide
Compressive strength

ABSTRACT

The method of determining the quantities of geopolymer concrete (GPC) ingredients to attain the required and specifiable characteristics is complex owing to the involvement of more variables compared with Portland cement concrete (PCC) systems. Therefore, this study evaluated the hydraulic responses and chemical resistance of GPC produced with supplementary cementitious materials (SCMs), ground granulated blast furnace slag (GGBFS) and corn cob ash (CCA) at ambient curing conditions. Corn cob was dehydroxylated at 600 °C and used as a partial replacement for GGBFS at 0, 20, 40, 60, 80, and 100%. The activators used were 12, 14 and 16 M concentration (M) of both sodium silicate (SS) and sodium hydroxide (SH). The chemical compositions of individual and mixed binders were analyzed, while the chemical moduli of each and blended binder were examined and evaluated based on the significant reactive oxides, hence resulting in the evaluation of reactivity indexes (RIs). Moreover, the compressive strength was predicted based on the RIs and mix design proportions (MDPs) of the blended concrete, while the durability properties of each concrete sample were investigated. The results indicated that the oxide compositions of GGBFS and CCA influenced the compressive strength of GPC produced. Compared with the experimental results, the predictive compressive strengths based on the RIs and the MDPs yielded a high precision with 95% "R^2". Furthermore, the incorporation of both GGBFS and CCA increased the durability of GPC produced against sulfate attacks. Ultimately, the model equations developed by this study can be beneficial in the refinement of mix designs of both GPC and conventional concrete incorporating SCMs provided the oxide compositions of the elements are obtained.

1. Introduction

Portland cement (PC) is the most commonly used binder in the production of Portland cement concrete (PCC). However, the production of Portland cement, apart from its negative impact on the environment, requires a massive industrial process [1,2]. Moreover, the global production of PC is responsible for both annual energy needs and yearly carbon dioxide (CO_2) emissions of up to 3 and 9%, respectively [3–5]. The yearly utilization of PCC in the construction industry is estimated to be 20 billion tons globally [6]. Furthermore, the need for the construction of infrastructures in fast-growing cities could emit 226 gigatonnes of CO_2 by 2050 in the developing nations [6]. Following this trend, the carbon budget of 800 gigatonnes of total CO_2 emissions targeted by the Paris Climate Agreement after 2017 would be challenging to achieve.

The growing awareness of the environmental impact associated with the production of the PC cannot be over-emphasized. The urgent need to reduce the emissions of CO_2 in the construction sector has been a top priority for a significant number of studies via

* Corresponding author.
E-mail address: solomon.oyebisi@covenantuniversity.edu.ng (S. Oyebisi).

https://doi.org/10.1016/j.conbuildmat.2020.119604
0950-0618/

the reduction in the utilization of PC or the investigation on fully or partially replaceable options for PC [7–9]. The commonly investigated method for reducing the use of PC is by the partial or full substitution of PC with SCMs. The SCMs are majorly industrial wastes, fly ash, coal ash, volcanic ash (VA), silica fume (SF), metakaolin (MK), and GGBFS; and agricultural residues, rice husk ash (RHA), corncob ash (CCA), cashew nutshell ash (CNSA), palm oil fuel ash (POFA), and bagasse ash (BA) [10–14]. Therefore, the practical and economical ways of improving concrete's suitability and, at the same time utilizing agro-industrial wastes is by the full or partial replacement of PC with SCMs [10]. The partial or fully incorporation of SCMs in the production of green concrete, apart from limiting the environmental impact of PCC, has been reported to improve the workability [15,16], mechanical [17–21], durability [22–25] and economical [26–28] properties of concrete. Moreover, the use of SCMs does not only reduce the initial CO_2 emissions of PC production but also reduce the volume of PCC needed in the construction industry and extend the service life of a building, which is typically based on the criteria of durability [29]. In 2016 and 2017 alone, the global production of corn was 969.69 and 1071.51 million metric tons, respectively [17]. However, most of the corncobs produced are disposed as waste, hence culminating in environmental pollution; this justified the recycling of CCA for GPC production.

The activity of any SCM can be evaluated using the concept of reactivity indexes (RIs) after the establishment of the oxide compositions [10,30–36]. Furthermore, the reactivity of any SCM is influenced by its oxide composition, mineralogical composition, fineness, and specific surface area [10,36–40]. Besides, type, mineralogical, and chemical compositions of aggregates influence the performance and reactivity of concrete [36,41,42]. However, a single oxide cannot be used to quantify the reactivity of SCM. Hence reactivity modulus (RM), hydraulic modulus (HM), and lime modulus (LM) are majorly applied to quantify the hydraulic or selfcementitious properties. In contrast, both silica modulus (SM) and alumina modulus (AM) are commonly used to determine pozzolanic properties [7,10,30–35].

Portland cement exhibits hydraulic reactions and possesses four significant phases such as alite (Ca_3SiO_5) and belite (Ca_3SiO_4), which give main strength and strong hydraulic results; aluminate ($Ca_3Al_2O_6$) and ferrite ($Ca_4Al_2Fe_2O_{10}$) offer minor strength and weakly hydraulic reactions [35,36]. In the same vein, GGBFS possesses a similar mineralogical composition to PC; it majorly comprises calcium oxide (CaO), silicon oxide (SiO_2), aluminium oxide (Al_2O_3), and iron oxide (Fe_2O_3), which give its hydraulic or selfcementitious properties [30,33]. As a result of high contents of magnesium oxide (MgO) and aluminium oxide (Al_2O_3), the major phases in slag materials are belite (Ca_3SiO_4), which gives main strength and strong hydraulic reactions; gehlenite ($Ca_2Al[AlSi]O_7$), which shows crystalline phases and gives low hydraulic properties, and generally inerts to water; akermanite ($Ca_2Mg[Si_2O_7]$) and merwinite ($Ca_3Mg[SiO_4]_2$) offer adsorption-active phases [30,33]. Besides, inorganic ashes such as RHA, CCA, and CNSA significantly contain lower content of CaO than either PC or GGBFS; this, in general, limits the hydraulic or selfcementitious properties of inorganic ashes [31,32]. The high contents of both SiO_2 and Al_2O_3 in some inorganic ashes show their potential in supporting the pozzolanic reactivity [31,32]. Moreover, the significant phases in inorganic ashes are mullite ($Al_6Si_2O_{13}$), which inerts to water and exhibits no hydraulic properties but only pozzolanic reactivity; and quartz (SiO_2), which provides the physical structure to resist chemical attacks and withstand exposure to extreme thermal conditions [31,32].

Demoulian et al. [43] reviewed and examined various indexes which exhibited the best prediction with compressive strength. The study revealed $(CaO + MgO + Al_2O_3)/SiO_2 > 1$ and $CaO/SiO_2 \leq 1.4$ as the best indexes. Behim et al. [33] investigated the reactivity of GGBFS using the chemical indexes, caustic soda test (CST), and slag activity index. It was discovered that the degree of reactivity of GGBGS strongly depends on its degree of fineness; the slag activity index increases with increasing fineness, hence recommending slag fineness of more than 350 cm^2/kg. Besides, CaO, SiO_2, Al_2O_3, Fe_2O_3, MgO, and SO_3 can be used to evaluate the chemical moduli of GGBFS. Also, unlike CST, slag activity index gave satisfactory values. In another study, Donatello et al. [44] compared strength activity index (SAI), frattini test (FT), and saturated lime test (SLT), to access the pozzolanic activity of silica fume (SF), metakaolin (MK), incinerated sewage sludge ash (ISSA), coal fly ash (CFA), and silica sand. The results showed ISSA and SF as the most reactive pozzolans after 1 day of SLT. However, MK, CFA, SF, and ISSA exhibited highly pozzolanic results after 7 days of SLT. Also, a strong correlation occurred between the SAI and FT results (R^2 = 86%), while SLT and SAI showed no correlation. Moreover, Xie and Visintin [10] developed a unified approach for modelling the mechanical strengths of concrete incorporating SCMs based on the mix design parameters and reactivity indexes. It was discovered that the reactivity indexes could be evaluated using the principal oxides, CaO, SiO_2, Al_2O_3, Fe_2O_3, MgO, and SO_3. These principal oxides guide the self-cementitious and pozzolanic reactions in the blended SCMs. It was also found that the water binding material ratio and the reactivity of SCMs significantly influenced the mechanical properties of the concrete mix. Oyebisi et al. [25] investigated the performance of cashew nutshell ash as a SCM in the production of concrete and modelled the compressive strength based on the reactivity indexes and mix design parameters of the blended concrete mix. It was found that the model of compressive strength following the RIs and mix design parameters of the mixed concrete, showed a significant relationship. Also, concrete mixed with CNSA resisted more sulfate attack than that of PCC.

Many standards have established the procedures of assessing the chemical indexes and hydraulic efficiency index of GGBFS [45,46], and the pozzolanic activity of pulverized fly ash or natural pozzolan [47–52]. ASTM C 989 [46] classifies GGBFS into three grades based on the mortar strength of slag activity index: Grades 80, 100, and 120. The slag activity index for grade 80 using 50% cement replacement by the mass of the binding materials must be 80% strength minimum of the reference-cement mortar at 28 days. Also, grade 100 must exhibit a slag activity index of more than 70 and 90% at 7 days and 28 days, respectively. The slag activity index for grade 120 must give a minimum of 90 and 110% strengths of the reference-cement mortar at 7 days and 28 days, respectively. Moreover, based on the caustic soda test in assessing the hydraulic activity of slag, ASTM C 1073–18 [53] recommends the compressive strengths ranging from 7 to 8 MPa and 12–15 MPa after 6 h and 8 h of hardening, respectively. On the other hand, BS 3892–1 [47] specifies a SAI greater than 0.80 as a positive pozzolanic activity for fly ash or natural pozzolan for 30% cement replacement after 7 and 28 days; in contrast, ASTM C 618 [52] recommends a SAI greater than 0.75 for 20% cement replacement after 7 and 28 days. However, the combination of GGBFS and CCA to GPC is a new development, as no study has been carried out to examine the sulfate attacks and the effects of activity indexes on the compressive strengths of slag-based GPC incorporating CCA.

This study aims to evaluate the oxide compositions of each binding material using the x-ray fluorescence analyzer (XRF); this guides in assessing the RIs of GGBFS-CCA based GPC using the RIs' concept. The durability of GGBFS-CCA based GPC was also investigated using the chemical attack systems. Finally, model equations were developed to predict the compressive strength of GGBFS-CCA based GPC following the RIs and MDPs.

2. Materials and methods

2.1. Materials

The locally sourced materials, GGBFS and CCA, as shown in Fig. 1, were used as SCMs for the production of GPC, while Portland limestone cement (PLC) was used as a binder for the production of PCC, and compared with GPC. Slag was ground to obtain GGBFS. Corncob was dehydroxylated at 600 °C for 3 h to obtain CCA. The SCMs were then sieved with BS 90 μm to obtain a similar fineness with PLC. The pH of the binding materials was measured following the procedure specified by BS 7755 [50]. GGBFS, CCA, and PLC showed a pH value of 9.83, 5.92, and 9.21, respectively. The specific gravity (SG) of the binding materials was determined following the requirements stated by BS EN 196-3 [54]. The results indicated 2.90, 2.44, and 3.15 g/cm^3 for GGBFS, CCA, and PLC, respectively. Owing to these results, GGBFS met the SG limit of 2.90–3.15 g/cm^3 specified by BS EN 15167-1 [45], while that of CCA confirmed the similar results obtained by Oyebisi et al. [11,21]. Moreover, the fineness of binding materials was determined using the dry sieving method, and BS sieve 90 μm as stipulated by BS EN 196-3 [54]. The results showed 7.6, 8.0, and 7.5% for GGBFS, CCA, and PLC, respectively, hence satisfying the 12% maximum fineness specification stated by BS EN 196-3 [54]. Therefore, the materials are suitable for use as binder and SCMs in concrete production. Furthermore, Laser diffraction, Model Beckman Coulter LS100, was used to analyze the particle size distribution of the binding materials, as shown in Fig. 2 over the range size of 0.5–900 μm. The results revealed a mean particle size of 20.68, 23.45, and 18.79 μm for GGBFS, CCA, and PLC, respectively. Besides, the specific surface area was carried out on the binding materials following the procedure stated by BS EN 196-3 [54] using the Blaine method at a standard porosity of 0.500. The results indicated 420, 625, and 375 m^2/kg for GGBFS, CCA, and PLC, respectively.

The alkaline solutions, SH pellets with 99% purity, and SS gel, which comprises Na_2O, SiO_2, and H_2O of 9.4, 30.1, and 60.5% respectively, with SiO_2/Na_2O weight ratio of 3.20 and S.G. of 1.40 g/cm^3 at 20 °C, were locally sourced and used as activators. A 354, 400, and 443 g of SH pellets were measured and dissolved in 646, 600, and 557 g of clean water conforming to BS EN 1008 [55] for the preparation of 12, 14, and 16 M activators, respectively [56]. Before casting, the solutions were prepared 24 h earlier to reduce the high rise in temperature owing to the reaction between SH pellets and water. For better performance, the SH solution was added to SS gel after 2 h using a SS/SH ratio of 2.5:1 [11,57–59].

The locally sourced aggregates (granites) were used and prepared at saturated dry surface conditions before the mix design. Grading was also conducted on the aggregates to obtain the needed particle size distribution (PSD). Moreover, the aggregates were characterized in line with the BS EN 12,620 [60]. The specific

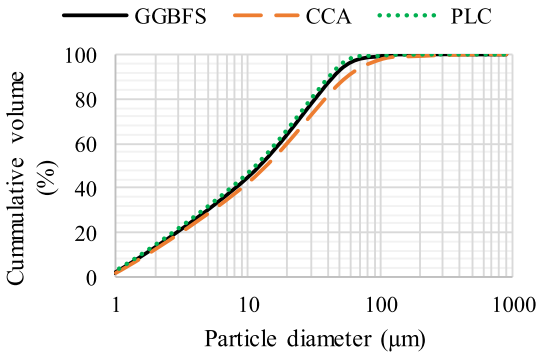

Fig. 2. The cumulative particle size distribution of binding materials used.

gravity (SG) and water absorption (WA) of aggregates were determined following the procedure stated in BS EN 12,620 [60]. The results showed the SG of 2.60 and 2.64 g/cm^3; and WA of 0.7 and 0.8% for both fine aggregate (FA) and coarse aggregate (CA), respectively. Besides, the moisture content (MC) was determined in consonance with BS EN 12,620 [60]. The results indicated the MC of 0.3 and 0.2% for both FA and CA, respectively. Fig. 3 shows the PSD of both FA and CA used; the aggregates satisfied the limits of BS EN 12,620 [60]. On the other hand, the mineralogical composition of the coarse aggregate (granite) was identified with the aid of the Petrological Microscope, Model RPI-3T. The sample was prepared, polished in a glass ground plate using a carborundum, and mounted on a clean glass slide with adhesive [41]. Also, the chemical composition was analyzed using the XRF spectrometer

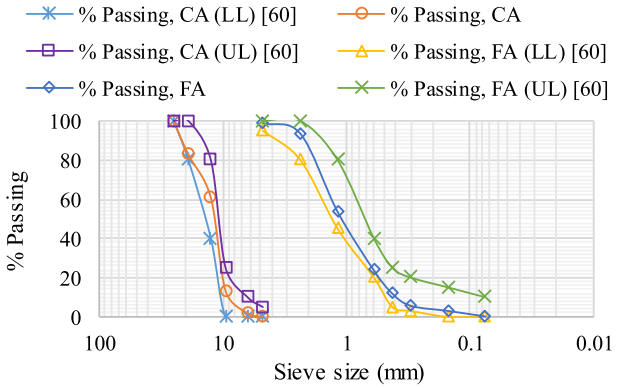

LL is the lower limit, UL is an upper limit, FA is fine aggregate, and CA is coarse aggregate

Fig. 3. The particle size distribution of aggregates used.

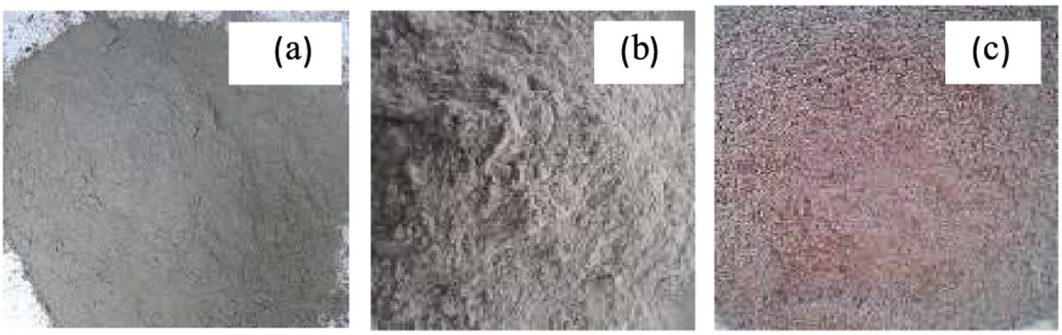

Fig. 1. Binding materials used (a) PLC (b) GGBFS (c) CCA.

machine, Philips PW-1800. The results of mineralogical composition showed quartz, feldspar, mica, and iron oxide of 62.50, 20.45, 16.55, and 0.50%, respectively. Moreover, the chemical composition revealed SiO_2, Al_2O_3, Fe_2O_3, CaO, MgO, SO_3, K_2O, Na_2O, P_2O_5, MnO, and LOI as 67.05, 14.40, 5.63, 3.90, 1.72, 0.02, 5.50, 1.16, 0.15, 0.05, and 0.52%, respectively. From these results, it is inferred that the coarse aggregate is acidic granite because the content of SiO_2 was in the range of 66–75% [41]. Besides, based on alkalinity, the granite was classified as calcalkalinity in that $(Na_2O + K_2O)^2/(SiO_2 - 43)$ was 1.85; this ranged between 1.2 and 3.5 for calcalkalinity [42]. XRF analysis was not performed on the FA because it comprises SiO_2 content, almost in its entirety [41,44].

2.2. Pozzolanic activity test methods

2.2.1. Strength activity index (SAI)

The SAI of CCA was determined in line with the BS 3892-1 [47]. The chemical composition of a pozzolanic material is important for its evaluation as a potential SCM. However, the most significance is its pozzolanic reactivity, because some pozzolanic materials or natural pozzolans may fail to exhibit this activity [34]. The SAI is commonly used to evaluate the pozzolanic characteristics of material: the reaction of pozzolan with lime, hence forming cementitious product [34]. Therefore, the SAI was determined for both 7 days and 28 days compressive strengths (CS) on the average of three samples using the relationship, as illustrated in Eq. (1) [47]. The cement-reference mortar cubes showed the CS of 40.64 and 50.43 MPa at 7 and 28 days, respectively. Following the formula, as illustrated in Eq. (1), the test pozzolan (CCA) exhibited a SAI of 0.85 and 0.91 at 7 and 28 days, respectively, thus showing considerable pozzolanic activity because SAI is greater than 0.80 recommended by BS 3892-1[47].

$$\text{SAI}, \% = \frac{P}{C} \times 100 \quad (1)$$

where P is the average CS of pozzolan-reference cement mortar cubes (MPa)

C is the average CS of reference-cement mortar cubes (MPa).

2.2.2. Frattini test (FT)

The FT was carried out following the procedure stated in BS EN 195-5 [48]. FT is a commonly used direct and chemical titration, which determines the dissolved Ca^{2+} and OH^- concentrations in a solution containing PC and the test pozzolan. However, every pozzolanic material with a strong acidic character does not show pozzolanic activity [34], and thus the evaluation of pozzolanic activity of a given material is a prerequisite for its use in cement and concrete production. Therefore, the theoretical maximum concentration (TMC) of [CaO] was determined using the relationship, as illustrated in Eq. (2) [48]. The sample, calcium concentration [CaO], was compared with the TMC [CaO] and the result was determined as the difference between the two values, hence expressing as a percentage of TMC removed, as shown in Table 1. Both SAI and FT were selected because they have been standardized, and widely used to determine the pozzolanic response of fly ash and metakaolin [44,47–49]. From Table 1, the results indicated that the pozzolanic activity of CCA is active with 51% lime removal.

$$\text{TMC[CaO]} = \frac{350}{[\text{OH}] - 15} \quad (2)$$

2.3. Hydraulic activity test (HAT) methods

2.3.1. Slag activity index

The method was carried out following the procedure in ASTM C 989 [46] for the GGBFS. The procedure is similar to that of SAI stated in BS 3892–1 [47] except for 50% cement replacement, C_3A content ranging from 6 to 10%, and a maximum of 3% SO_3 content specified by the standards for the reference cement [45,46]. Therefore, from the XRF results, PLC exhibits 2.03% SO_3 content, hence satisfying the maximum requirement of 3%. Besides, C_3A was quantified based on Bogue's equation, as shown in Eq. (3) [36]. Based on the XRF result and in line with Eq. (3), the result exhibited 10% C_3A, thus fulfilling the maximum specification of 10%. Finally, the slag activity index was determined following the relationship, as illustrated in Eq. (1).

$$C_3A = 2.65(Al_2O_3) - 1.69(Fe_2O_3) \quad (3)$$

The CS of GGBFS-reference cement mortar cubes to the cement-reference mortar cubes with the mean particle size (d_v50 = 20.68 μm) showed the slag activity index of 76.42 and 98.53% at 7 and 28 days, respectively, hence classifying as grade 100 because the activity index is more than 70 and 90% at 7 and 28 days, respectively [46].

2.3.2. Caustic soda test (CST)

This method was carried out by the procedure outlined in ASTM C 1073-18 [53] by mixing 200 g NaOH solution with 800 g distilled water, thus forming a litre of diluted solution. The diluted solution-to-GGBFS ratio was fixed at 0.5 and used to prepare 40 mm × 40 mm × 160 mm prismatic samples. After 6 and 24 h, all samples were demoulded and tested for CS. The results, average of three test samples, indicated 7.63 and 14.52 MPa at 6 and 8 h, respectively, hence satisfying the specifications of 7–8 MPa and 12–15 MPa after 6 and 8 h, respectively, recommended by ASTM C 1073–18 [53]. The slag activity index and CST were adopted because they have been standardized and offered satisfactory results [33,43,45,46].

2.4. Materials characterization

The oxide compositions of binding materials, CCA, GGBFS, and PLC, were analyzed using the XRF spectrophotometer machine, Philips PW-1800. The results are shown in Fig. 4. The results reveal that CCA satisfied the chemical pozzolanic requirements stipulated by BS EN 450-1 [61] and BS EN 8615-2 [62] such that the addition of SiO_2, Al_2O_3, and Fe_2O_3 met 70% minimum requirement. The content of CaO within the range of 10–20% established by Al-Akhras [63] was also met. Owing to these results, it can be deduced that the CCA could exhibit a pozzolanic reaction and used as the SCM in the production of blended GPC. On the other hand, GGBFS met the BS EN 15167-1 [45]'s limit requirements of 32–40% for both silica (SiO_2) and lime (CaO) contents. The chemical moduli of $(CaO + MgO/SiO_2) \geq 1$, $(CaO/SiO_2) \leq 1.4$, and $SiO_2 + CaO + MgO \geq 67\%$ stipulated by BS EN 15167–1 [45] were also met. Also, the oxide compositions obtained herein for GGBFS show similar compositions with the previous studies [15,16,57,58]. Therefore, an inference is made that GGBFS utilized in this study could exhibit both pozzolanic and self-cementitious reactivity, hence suitable

Table 1
Eight days FT results for two test materials determined using Eq. (2).

Sample	[OH] mmol l^{-1}	[CaO] mmol l^{-1}	TMC [CaO] mmol l^{-1}	[CaO] reduction (%)
Control	56.83	8.25	8.37	0.70
CCA	39.72	4.63	14.16	50.72

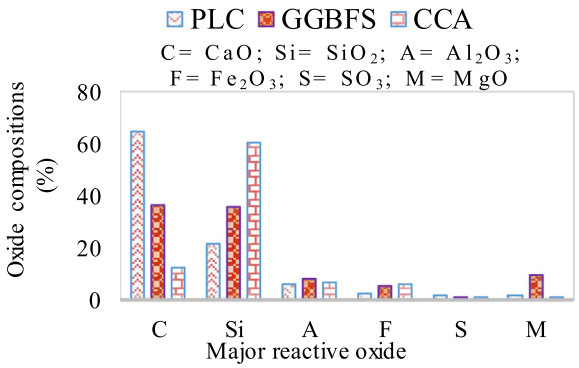

Fig. 4. Chemical compositions of binding materials used.

for use. In the same vein, the PLC fulfilled the chemical requirements specified by BS EN 196-2 [64].

The microstructural behaviour of the binding materials, GGBFS, CCA, and PLC, was examined using the SEM machine, JEOL 7000600, to establish the characteristics that influenced the RIs of each binder. The SEM analysis was performed on a flat (general) scan. For the analysis, the accelerated voltage was constant at 15 kV, while images were observed at 4000x magnification in a high vacuum. The SEM micrographs, as shown in Fig. 5, reveal that the internal structure of PLC, to a limited extent, was wrinkled, and the particles were angular in shape with sharp needles. However, the GGBFS particles revealed an amorphous structure. Moreover, the internal structure of CCA showed that the particles were crystalline and spherical. Therefore, it is inferred that the particle shapes of these binding materials influenced the reactivity of each and blended binder produced [29,30].

2.5. Mix design quantities

The mix quantities were designed following the procedures stated by BS EN 206 [65]. The percentage replacement of GGBFS by CCA was selected based on the applicable studies [16,19] to examine the replacement levels, which would meet the target strengths for both structural and non-load bearing applications. Owing to this, GGBFS was replaced with CCA at 0, 20, 40, 60, 80, and 100% for the production of GPC and was respectively indicated as N1, N2, N3, N4, N5, and N6, while the PCC (100% PLC) was indicated as N0. The mix was designed to attain target strengths 30 MPa and 40 MPa for grades M 30 and M 40 concrete, respectively. Besides, the broad and wider use of M 30 and M 40 in construction sector informed the selection of these concrete grades as mix design proportions. The mix design quantities for both M 30 and M 40 are shown in Tables 2 and 3, respectively.

2.6. Mix preparation, casting and curing

The dry constituents were prepared following the procedures stated by BS 1881-125 [66] and BS EN 12390-2 [67]. The fresh concrete was poured into a standard cubical mould of 150 mm, randomly compacted each in three layers, cured under 25 °C and 65% RH, and tested at 7, 28, 56, and 90 days.

2.7. Experimental tests and analysis

2.7.1. Mechanical test

The compressive strength (f_c) was determined with the aid of an INSTRON 5000R UTM following the procedures stated by BS EN 12390-4 [68] in a constant force regime under a loading rate of 0.6 MPa per second. For each mix ID, a total of three (3) samples were crushed, and the average of the three values was obtained and used for the analysis.

2.7.2. Reactivity indexes (RIs) of binding materials

The RIs of binding materials were evaluated using the principal reactive oxides such as CaO, SiO_2, Al_2O_3, Fe_2O_3, MgO, and SO_3 following the establishment of their oxide compositions, which reflect both self-cementitious and pozzolanic reactivity

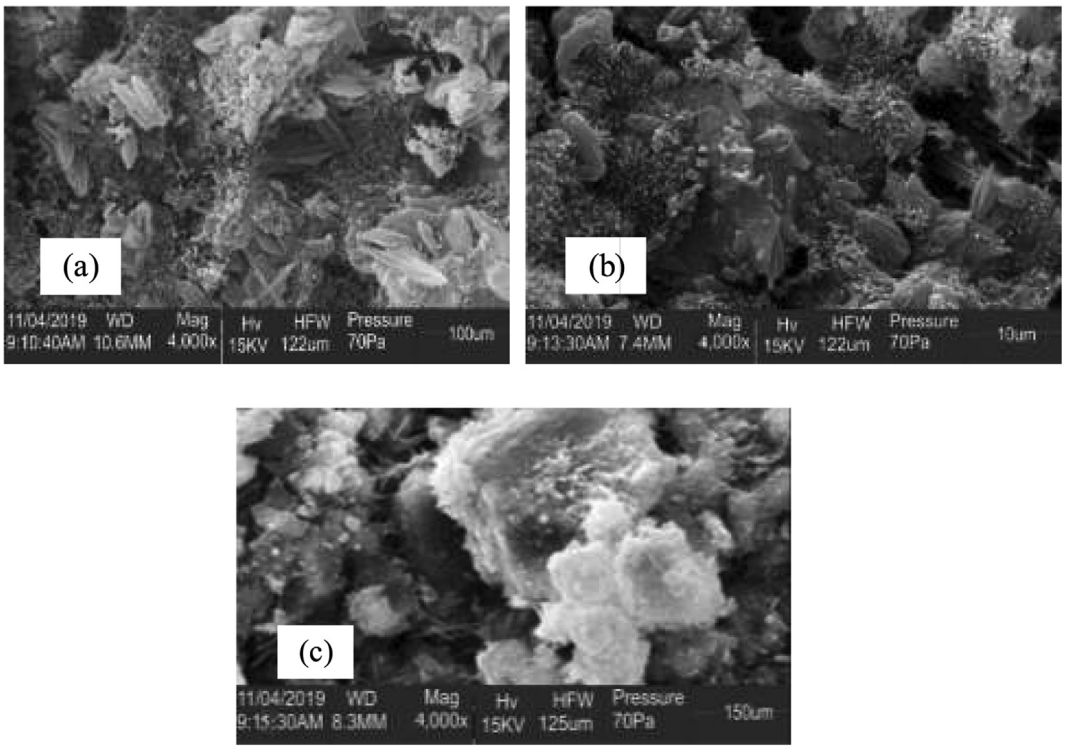

Fig. 5. SEM micrographs on binding materials. (a) PLC (b) GGBFS (c) CCA.

Table 2
Mix quantities for M 30 (in Kg/m^3).

Mix ID	PLC	GGBFS	CCA	FA	CA	SH	SS	SS/SH
N0	390	0	0	675	1031	0	0	0
N1	0	390	0	675	1031	60	150	2.5
N2	0	312	78	675	1031	60	150	2.5
N3	0	234	156	675	1031	60	150	2.5
N4	0	156	234	675	1031	60	150	2.5
N5	0	78	312	675	1031	60	150	2.5
N6	0	0	390	675	1031	60	150	2.5

Water to binder (w/b) ratio = 0.54.
Binder to aggregate ratio (b/agg) ratio = 0.23.

Table 3
Mix quantities for M 40 (in Kg/m^3).

Mix ID	PLC	GGBFS	CCA	FA	CA	SH	SS	SS/SH
N0	500	0	0	585	1031	0	0	0
N1	0	500	0	585	1031	60	150	2.5
N2	0	400	100	585	1031	60	150	2.5
N3	0	300	200	585	1031	60	150	2.5
N4	0	200	300	585	1031	60	150	2.5
N5	0	100	400	585	1031	60	150	2.5
N6	0	0	500	585	1031	60	150	2.5

Water to binder (w/b) ratio = 0.42.
Binder to aggregate ratio (b/agg) ratio = 0.31.

[10,25,31–34,43,45]. The concept which guides the RIs is illustrated in Eq. 4–8 as RM, HM, LM, SM, and AM of each and mixed binders, respectively.

$$RM = \frac{CaO + MgO + Al_2O_3}{SiO_2} \quad (4)$$

$$HM = \frac{CaO}{SiO_2 + Al_2O_3 + Fe_2O_3} \quad (5)$$

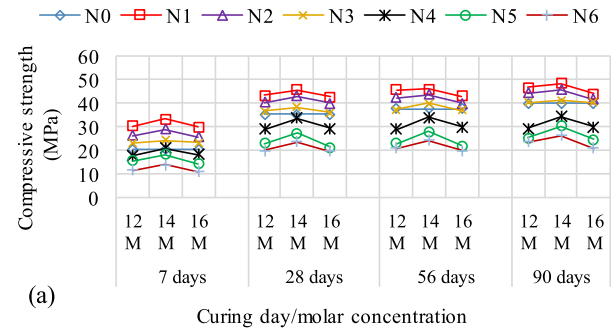

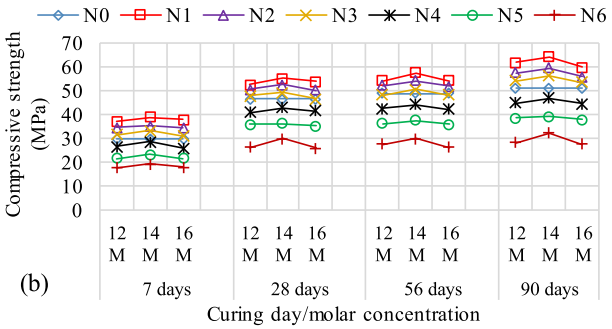

N0 (100% PLC); N1 (100% GGBFS); N2 (80% GGBFS + 20% CCA); N3 (60% GGBFS + 40% CCA); N4 (40% GGBFS + 60% CCA); N5 (20% GGBFS + 80% CCA); and N6 (100% CCA)

Fig. 6. Compressive strengths for (a) M 30 and (b) M 40.

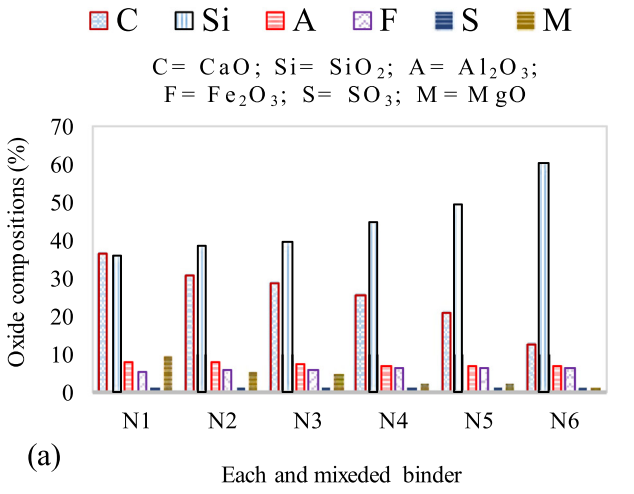

N1 (100% GGBFS); N2 (80% GGBFS + 20% CCA); N3 (60% GGBFS + 40% CCA); N4 (40% GGBFS + 60% CCA); N5 (20% GGBFS + 80% CCA); and N6 (100% CCA)

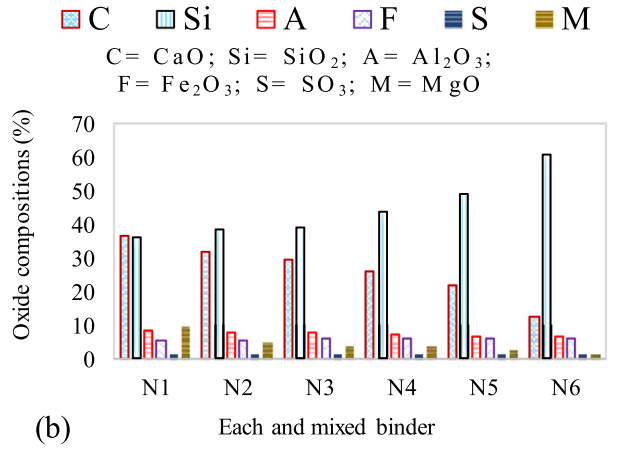

Fig. 7. Principal reactive oxides of each and mixed binder for (a) M 30 and (b) M 40.

$$LM = \frac{1.0CaO - 0.7SO_3}{2.8SiO_2 + 1.1Al_2O_3 + 0.7Fe_2O_3} \quad (6)$$

$$SM = \frac{SiO_2}{Al_2O_3 + Fe_2O_3} \quad (7)$$

$$AM = \frac{Al_2O_3}{Fe_2O_3} \quad (8)$$

2.7.3. Prediction of compressive strength (f_c) based on RIs, w/b ratio, and b/agg ratio

Either RM, HM, or LM quantified the self-cementitious properties of each and mixed binding material while the pozzolanic activity was quantified by both SM and AM [7,10,24,25,31–35,69,70]. Owing to this, a linear relationship exists in the prediction of fc and RIs. Thus, the regression was first modelled based on the combination of RM, SM, and AM; HM, SM, and AM; and LM, SM, and AM using the statistical software. Furthermore, in determining the fc of blended concrete, the RIs of blended binders were integrated and normalized with an inverse of water to binder (w/b) ratio; hence, fc becomes a direct proportion to RIs, but an inverse proportion to w/b ratio [10,24,25]. In this study, alkaline solutions were prepared and used as activators in the dose of 12–16 M activators. Therefore, the fit regression relationship between fc and w/b ratio was first normalized and modelled in the range of 0.54–0.42 w/b ratio for M 30-M 40 concrete, respectively. Predicting the parameters in Minitab 17, the values of f_c was set as a response (dependent variable), while the values of RIs were selected as continuous predictors (independent variables).

The binder to aggregate (b/agg) ratio also contributed a vital role to the evaluation and improvement of the concrete strength apart from RIs and w/b ratio [10,25,36,71,72]. The fc of blended binders was significantly improved when RIs, w/b ratio, and b/agg were all used for the strength correlation [10,25]. It is noteworthy to state that the volume ratio was used to model the b/agg ratio against the weight ratio. For each mix, the volume fraction was determined using its moisture content and specific gravity to improve the binder-aggregate packing capacity [10]. Following the incorporation of w/b ratio, the fit regression relationship between fc and b/agg ratio was modelled in the range of 0.29–0.23b/agg ratio for M 30-M 40 concrete, respectively. Owing to this, f_c was predicted based on the RIs, w/b ratio and b/agg ratio as illustrated in Eq. 9–11.

$$f_c = \beta + \left(\frac{\alpha_1 RM + \alpha_2 SM + \alpha_3 AM}{w/_b}\right)\left(b/_{agg}\right) \quad (9)$$

$$f_c = \beta + \left(\frac{\alpha_1 HM + \alpha_2 SM + \alpha_3 AM}{w/_b}\right)\left(b/_{agg}\right) \quad (10)$$

$$f_c = \beta + \left(\frac{\alpha_1 LM + \alpha_2 SM + \alpha_3 AM}{w/_b}\right)\left(b/_{agg}\right) \quad (11)$$

where β, α_1, α_2, α_3 are the magnitudes of coefficients.

2.7.4. Durability test

The chemical resistance tests were performed on the selected concrete samples following the procedures stated in Neville [36], Singh et al. [73], and BS EN 16523-1 [74] using the solutions of magnesium sulfate ($MgSO_4$) at 5% concentration for sulfate attacks. The concrete specimens were tested for both weight and strength loss after 90 days immersion in $MgSO_4$.

3. Results and discussion

3.1. Compressive strength (CS)

Fig. 6 indicates the CS of the GGBFS-CCA based GPC. The results revealed that the CS increased with increasing GGBFS content in the blended mix for both M 30 and M 40 at all levels of alkaline activators. The reason for the increase in CS cannot be far-fetched: during the dissolution process, the glassy phase of aluminosilicate gel in GGBFS reacts with alkaline activators, hence resulting in x-ray amorphous aluminosilicate gel (X-RAAG). The X-RAAG, according to Chen and Brouwers [17], is responsible for the cementitious matrix and hydraulic characteristics of the composite mix, which effects higher mechanical strength in the GPC. However, unlike 12 and 14 M activators, 16 M activator exhibited the lowest CS; and this factor could be attributed to the fact that OH^- cation, at 16 M activation, has exceeded its saturation point, consequently, unreacted OH^- cation becomes hindrance to strength gain rather than a benefit [15].

3.2. Principal reactive oxides of blended binders

Fig. 7 shows a decrease in CaO, Al_2O_3, and MgO contents with increasing CCA content, while SiO_2, Fe_2O_3, and SO_3 contents increase with increasing CCA content in the blended mix. The reason for the increase could be attributed to the higher specific surface area of CCA compared with GGBFS: this allows CCA to fill more volume in the mix, hence increasing SiO_2, Fe_2O_3, and SO_3 contents, which are predominantly present in CCA; and decreasing CaO, Al_2O_3, and MgO contents, which are much greater in GGBFS, as

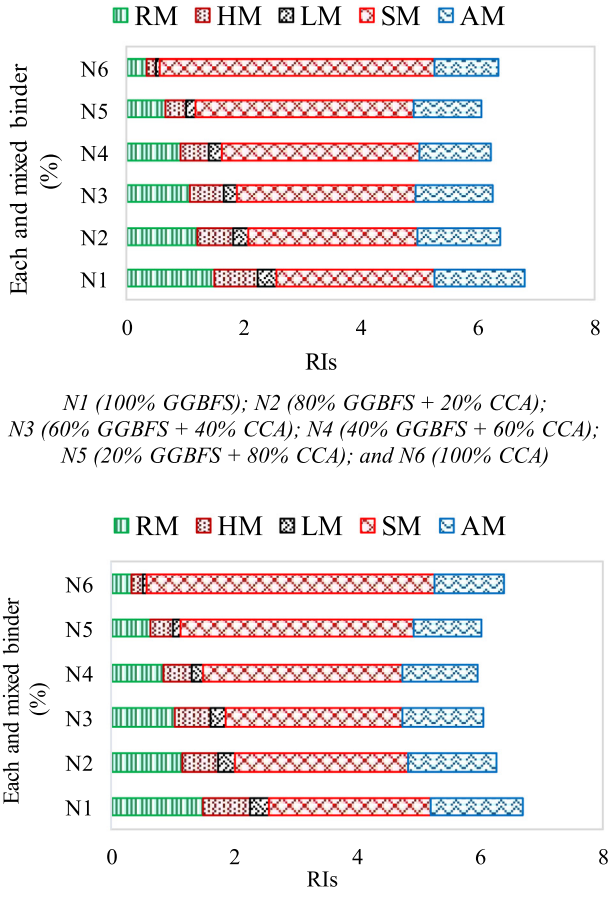

N1 (100% GGBFS); N2 (80% GGBFS + 20% CCA); N3 (60% GGBFS + 40% CCA); N4 (40% GGBFS + 60% CCA); N5 (20% GGBFS + 80% CCA); and N6 (100% CCA)

Fig. 8. RIs of each and mixed binders for. (a) M 30 and (b) M 40.

shown in Fig. 4. Besides, the similar findings reported by Akinwumi and Aidomoje [75] revealed that the reactive oxides, CaO, MgO, and Al_2O_3 decrease with the increase in CCA content; in contrast, SiO_2, Fe_2O_3, and SO_3 increase with increasing CCA content for the CCA-PC blend. Meanwhile, Behim et al. [34] and Demoulian [43] stated that GGBFS exhibits a similar mineralogical composition to PC, it majorly possesses oxides of Ca, Si, Al, Mg, and Fe, and this gives GGBFS its hydraulic and pozzolanic properties. Also, Xia and Visintin [10] and Darquennes [30] opined that slag is said to exhibit both self-cementitious and pozzolanic properties if the content of CaO and SiO_2 is higher than 30%. From the XRF results of GGBFS, it is clear that the contents of both CaO and SiO_2 are higher than 30%. On the other hand, Taylor [76] and Hewlett [77] reported that the self-cementitious reaction of slag decreases as the crystalline content in the blended mix increases. This demonstrates that the reactivity of GGBFS depends on the increasing content of its amorphous structure, and the significant oxides which contribute to the high phase of an amorphous structure are oxides of Ca, Al, and Mg [78,79]. Thus, through close examination of microstructures of binding materials, as shown in Fig. 5, it was evident that the content of the amorphous structure in GGBFS could gradually decrease, while the content of the crystalline structure in CCA might increase when GGBFS is replaced with CCA. Consequently, as the content of CCA in the blended mix increases, CaO, Al_2O_3, and MgO in GGBFS decrease, while SiO_2, Fe_2O_3, and SO_3 in CCA increase; this affirms the findings from relevant studies such that the reactivity of GGBFS increases with increasing CaO, MgO, and Al_2O_3 contents but reduces as the contents of SiO_2, Fe_2O_3, and SO_3 in the blended mix increase [80–83]. However, it was pointed out that GGBFS comprises small crystal material and is advantageous to its reactivity [84–86]. Besides, Gruskovanjak et al. [87] pointed out that the optimum content of the principal reactive oxides of slag is more beneficial to its selfcementitious reactivity than the content of the amorphous structure. Therefore, it is inferred that the contents of CaO, Al_2O_3, MgO, SiO_2, Fe_2O_3, and SO_3 influence the reactive potentials of GGBFS-CCA blended binders.

3.3. Ris of the blended mix

In assessing the RIs of each mixed binder, Eq. 4–5 was used, and the results are shown in Fig. 8. It was revealed that the RM, HM, LM, and AM decreased with increasing CCA content, while the SM increased with increasing CCA content in the blended mix for both M 30 and M 40. The reason for a decrease in RIs as the CCA content increase in the mix is associated with the decrease in hydraulic/self-cementitious properties of GGBFS content as more CCA is added, because CCA exhibits pozzolanic activity rather than hydraulic reactivity, which gives material its self-cementitious characteristics. Besides, it was evident from the results that CaO, Al_2O_3, MgO, SiO_2, Fe_2O_3, and SO_3 influenced the RIs of the blended binders. The RM, HM, and LM of the blended binders increased with increasing CaO, Al_2O_3, MgO contents, while the SM and AM of the blended binders increased as the contents of SiO_2 and Al_2O_3 increased, respectively. In contrast to HM, the RM of the blended binders met the minimum requirement of 1.0 specified by BS EN [62]. However, the LM of the blended binders was not satisfied with the minimum range of $\geq 0.66 \leq 1.02$, recommended by BS EN [61]. This can be attributed to the fact that the ratio of the

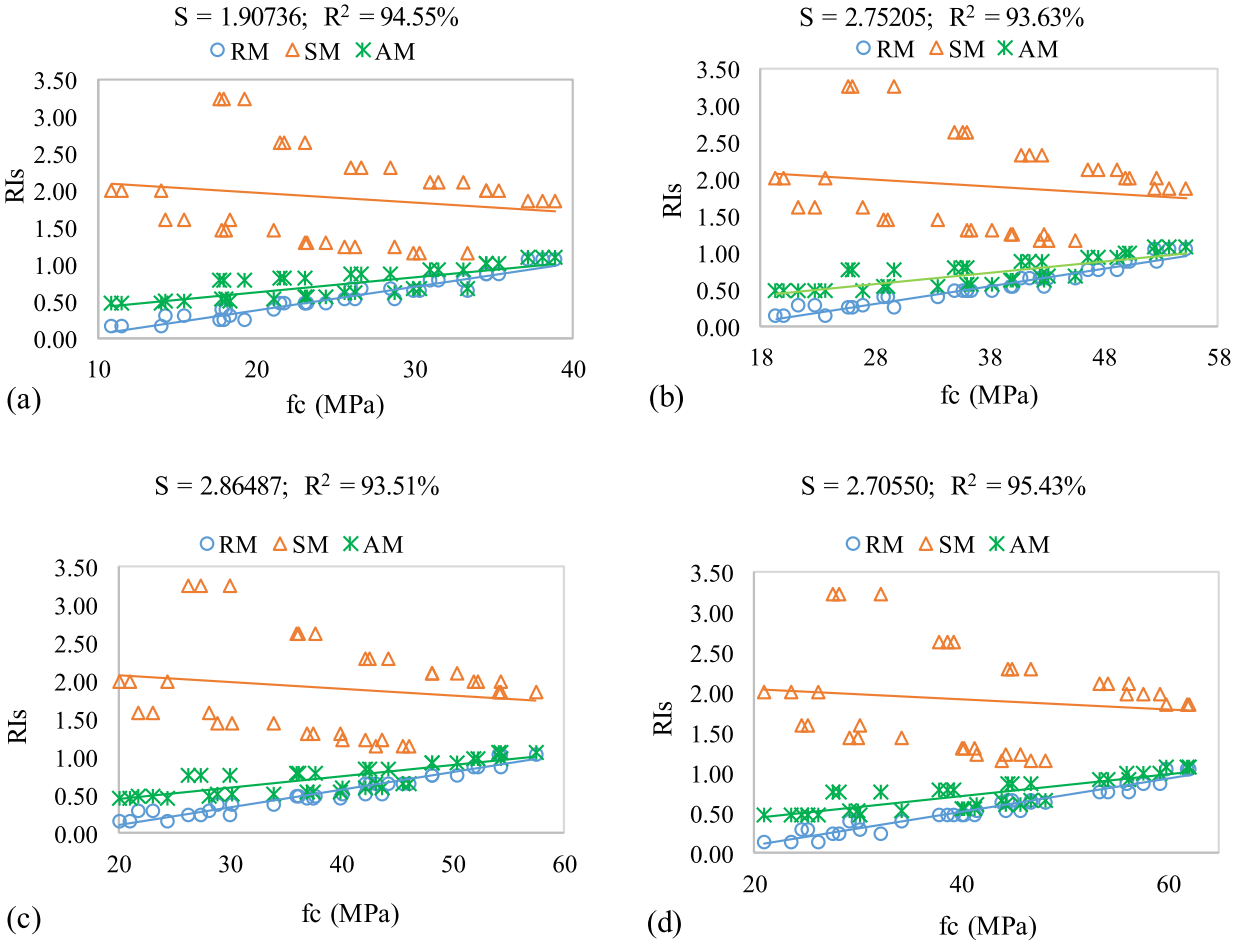

Fig. 9. Statistical data for RM, AM, SM, w/b ratio, and b/agg ratio (a) 7 (b) 28 (c) 56 and (d) 90 days.

lime content to the silica, aluminate, and ferrate contents is low in GGBFS-CCA blended binders compare with PC binder incorporating SCMs. Statistically, the RM, HM, LM, and AM of the blended mix increase from 25 to 78%, 19–77%, 19–77%, and 11–26% as the percentage replacement of CCA by GGBFS increases from 20 to 100% for both M 30 and M 40, respectively. The self-cementitious properties of blended binders increase with an increase in CaO, Al_2O_3, and MgO contents, thus resulting in stronger hydraulic reactions [33,88]. Owing to these, the decrease in RIs may be attributed to the reduction in principal reactive oxides, CaO, Al_2O_3, and MgO as a result of the increase in CCA content in the blended mix. However, there was a decrease in SM of the blended mix from 44 to 10% as the percentage replacement of CCA by GGBFS rose from 20 to 100% for both M 30 and M 40, respectively. Meanwhile, as shown in Fig. 7, CCA, being a pozzolan, exhibits higher content of silica (SiO_2) compare with that of GGBFS. Therefore, this result confirms the findings reported by Mathhes et al. [86] that SM increases with increasing SiO_2 content, hence resulting in stronger pozzolanic properties. On the other hand, the reactivity of GGBFS depends on its amorphous structure, thus influencing its RIs [85,86]. This assertion confirms the SEM micrographs, as shown in Fig. 5 (b) and (c) for GGBFS and CCA, which respectively display amorphous and crystalline structures.

3.4. Prediction of compressive strength (f_c) based on RIs, w/b ratio, and b/agg ratio

3.4.1. Prediction of fc based on RM, AM, SM, w/b ratio, and b/agg ratio

Following the Eq. (9), the results of the statistical data are presented in Fig. 9 (a)-(d) for 7, 28, 56, and 90 days, respectively. From Fig. 9, it is observed that some data points of SM significantly deviated from the regression line; this may be asserted to the diversity of chemical compositions of mixed binders, aggregate texture, shape, and volume, and mix design proportions; this assertion confirms the findings reported by Xie and Visintin [10] and Neville [36] that differences in the oxide composition of blended binders, aggregate types, and methods of mix design affect the data results, hence influencing the reactive potentials of blended concrete incorporating SCMs. Moreover, it was noticed that the compressive strength of GGBFS-CCA based concrete increases with increasing RM and AM but decreasing SM; this may be attributed to the higher contents of CaO and Al_2O_3 in GGBFS, which increases RM and AM, thus resulting in a stronger self-cementitious reaction. However, the higher content of SiO_2 in CCA increases its SM, hence leading to a pozzolanic reaction rather than a hydraulic reaction. Besides, it confirms the findings of a similar study reported by Gruskovnjak et al. [82] that the RM and AM increase as the CaO and Al_2O_3 contents increase, while SiO_2 content reduces, thus resulting in high reactivity. However, the higher contents of SiO_2 and low contents of CaO and Al_2O_3 result in low reactivity. On the other hand, a blended mix with high contents of CaO, Al_2O_3, and MgO exhibits high self-cementitious properties in the presence of alkaline activators [80,81,84,86].

The fit regression model was used for the correlation of fc based on the RIs (RM, AM, and SM), w/b ratio, and b/agg ratio at the global trend of 95% confidence interval (CI) and prediction interval (PI). Thus, the regression equations are illustrated in Eq. 12–15 for 7, 28, 56, and 90 days, respectively. From the regression analysis, the coefficients of determination (R^2) are 94.55, 93.63, 93.51, and 95.43% fit to predict the data at 95% CI and PI for 7, 28, 56, and 90 days, respectively.

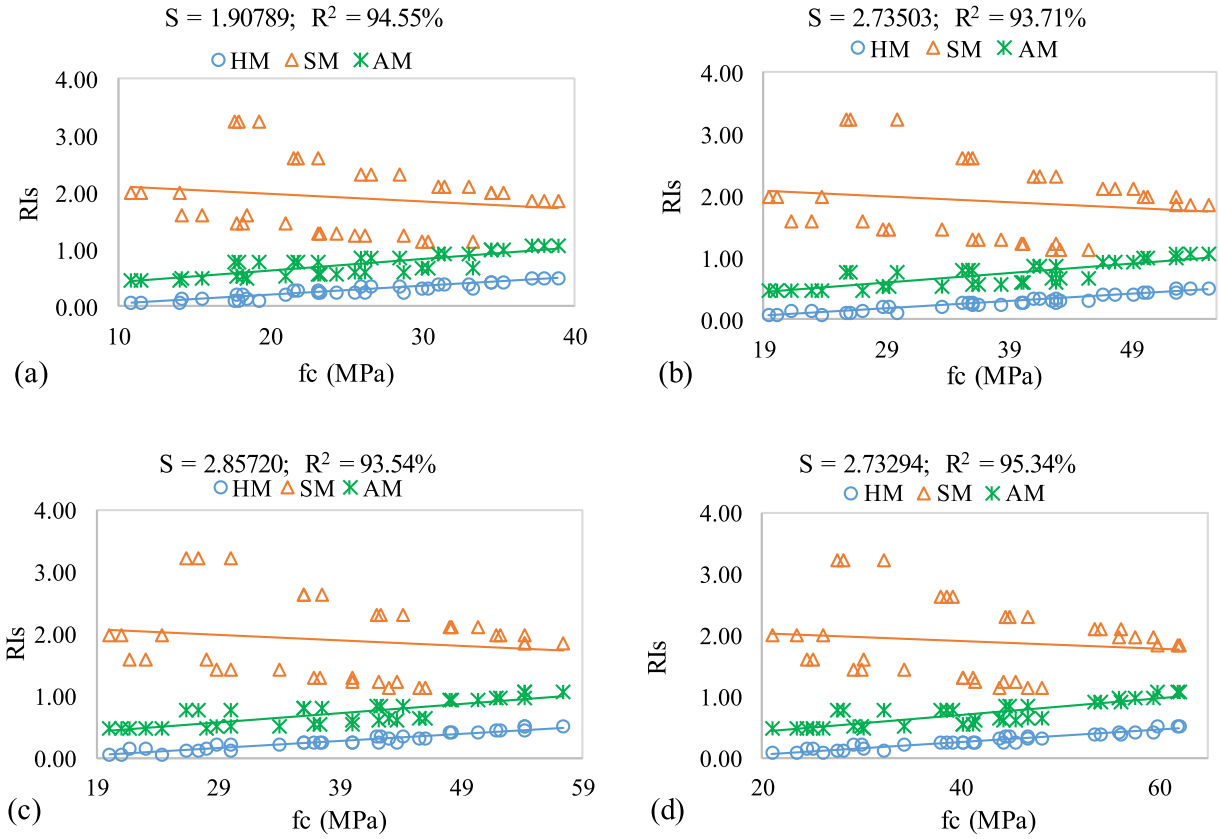

Fig. 10. Statistical data for HM, AM, SM, w/b ratio, and b/agg ratio (a) 7 (b) 28 (c) 56 and (d) 90 days.

$$f_{C-7days} = \left\{\frac{71.80AM - 13.49SM - 21.70RM}{\frac{w}{b}}\right\}\left(\frac{b}{agg}\right) + 10.45 \quad (12)$$

$$f_{C-28days} = \left\{\frac{56.80AM - 10.68SM - 1.30RM}{\frac{w}{b}}\right\}\left(\frac{b}{agg}\right) + 17.74 \quad (13)$$

$$f_{C-56days} = \left\{\frac{64.90AM - 12.12SM - 5.90RM}{\frac{w}{b}}\right\}\left(\frac{b}{agg}\right) + 18.09 \quad (14)$$

$$f_{C-90days} = \left\{\frac{94.40AM - 16.88SM - 21.10RM}{\frac{w}{b}}\right\}\left(\frac{b}{agg}\right) + 16.65 \quad (15)$$

3.4.2. Prediction of fc based on HM, AM, SM, w/b ratio, and b/agg ratio

Fig. 10 (a)-(d) indicate the statistical data for HM, AM, SM, w/b ratio, and b/agg ratio at 7, 28, 56, and 90 days, respectively. It was noticed that some data points of SM were out of the regression line due to the difference in oxide compositions of the blended binders, the volume and chemical compositions of aggregates, and mix proportions. Also, the compressive strength of GGBFS-CCA based concrete increased with increasing HM and AM but decreasing SM. The reason for a higher strength as a result of an increase in HM and AM cannot be far-fetched: GGBFS exhibits higher content of CaO and Al_2O_3, compare with CCA, hence resulting in stronger hydraulic reaction, but this hydraulic reaction decreases when replaced with CCA, which predominantly contains a higher content of SiO_2. This supports the findings reported in various studies that the hydraulic response of slag reduces with increasing silica content 76–79]. Therefore, it is inferred that the HM of GGBFS-CCA blended binder increases with higher contents of CaO and Al_2O_3 and the lower content of SiO_2 in the mix.

The fit regression model was used for the correlation of fc based on the RIs (HM, AM, and SM), w/b ratio, and b/agg ratio at the 95% CI and PI, and the regression equations are illustrated in Eq. 16–19 for 7, 28, 56, and 90 days, respectively. From the regression analysis, R^2 is 93.06, 93.71, 93.54, and 95.34% fit to predict the data at 95% CI and PI for 7, 28, 56, and 90 days, respectively.

$$f_{C-7days} = \left\{\frac{55.20AM - 10.39SM - 20.30HM}{\frac{w}{b}}\right\}\left(\frac{b}{agg}\right) + 10.44 \quad (16)$$

$$f_{C-28days} = \left\{\frac{41.10AM - 8.42SM + 15.70HM}{\frac{w}{b}}\right\}\left(\frac{b}{agg}\right) + 17.58 \quad (17)$$

$$f_{C-56days} = \left\{\frac{48.30AM - 9.14SM + 12.00HM}{\frac{w}{b}}\right\}\left(\frac{b}{agg}\right) + 17.92 \quad (18)$$

$$f_{C-90days} = \left\{\frac{63.00AM - 11.15SM + 2.40HM}{\frac{w}{b}}\right\}\left(\frac{b}{agg}\right) + 16.42 \quad (19)$$

3.4.3. Prediction of fc based on LM, AM, SM, w/b ratio, and b/agg ratio

The statistical data for LM, AM, SM, w/b ratio, and b/agg ratio are presented in Fig. 11 (a)-(d) for 7, 28, 56, and 90 days, respectively. It was observed that some data points of SM were out of the global trend due to the diversity in oxide compositions, the

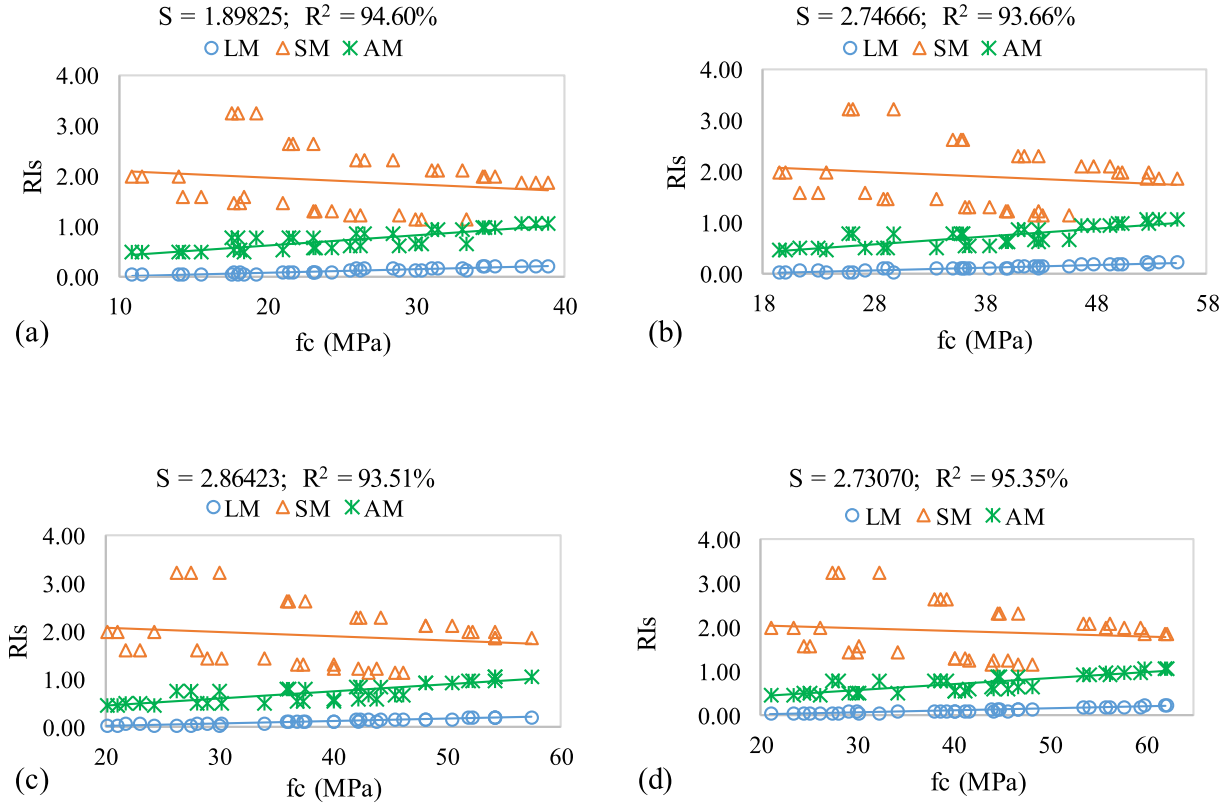

Fig. 11. Statistical data for LM, AM, SM, w/b ratio, and b/agg ratio (a) 7 (b) 28 (c) 56 and (d) 90 days.

volume of aggregates, and mix proportions of the blended binders. Moreover, the compressive strength of GGBFS-CCA blended concrete increases with increasing LM and AM but decreasing SM; this may be attributed to the fact that GGBFS exhibits higher content of CaO and Al_2O_3 compared with CCA, hence resulting in a stronger reactive component. Still, this reactive component decreases when replaced with CCA, which majorly contains a higher content of silica. Therefore, it is inferred that the LM of GGBFS-CCA blended binder increases with higher contents of CaO and Al_2O_3 and the lower content of SiO_2 in the mix.

The fc, RIs (LM, AM, and SM), w/b ratio, and b/agg ratio was predicted using the fit regression model at the 95% CI and PI, and the regression equations are illustrated in Eq. 20–23 for 7, 28, 56, and 90 days, respectively. From the regression analysis, R^2 is 94.60, 93.66, 93.51, and 95.35% fit to predict the data at the global trend for 7, 28, 56, and 90 days, respectively.

$$f_{C-7days} = \left\{\frac{58.600AM - 11.24SM - 56.20LM}{\frac{w}{b}}\right\}\left(\frac{b}{agg}\right) + 10.54 \quad (20)$$

$$f_{C-28days} = \left\{\frac{48.10AM - 9.02SM + 22.20LM}{\frac{w}{b}}\right\}\left(\frac{b}{agg}\right) + 17.61 \quad (21)$$

$$f_{C-56days} = \left\{\frac{51.70AM - 9.67SM + 15.80LM}{\frac{w}{b}}\right\}\left(\frac{b}{agg}\right) + 17.95 \quad (22)$$

$$f_{C-90days} = \left\{\frac{69.40AM - 12.36SM - 15.30LM}{\frac{w}{b}}\right\}\left(\frac{b}{agg}\right) + 16.53 \quad (23)$$

3.4.4. Comparison of experimental results with predictive values

Figs. 12 and 13 illustrate the statistical comparison and trend between the compressive strengths of experimental results and that of predictive models for M 30 and M 40, respectively. It was observed that both experimental and predictive results exhibited similar values and patterns of compressive strength. In contrast to HM, both LM and RM showed the best fit at all levels of curing time for both M 30 and M 40. These observations confirm the findings reported in similar studies such that LM yields the best fit for PC blended with cashew nutshell ash (CNSA) [25], while RM yields the best fit for blended concrete incorporating SCMs [10]. Despite the similar values and trends, it was observed that LM of the GGBFS-CCA blended binders was lowered compared with the minimum requirements ($\geq 0.66 \leq 1.02$) recommended by BS EN 197-1 [89]; HM was less than 1 compared with the minimum requirement (> 1) specified by BS EN 197-1 [89], but RM satisfied the minimum requirement (> 1) specified by Behim et al. [33], Demoulian et al. [43], and BS EN 15167-1 [45]. The variations in LM and HM may be attributed to the difference in chemical compositions of blended binders in that BS EN 197-1 [89]'s recommendation was based on the PC mixed binders such that the ratio of CaO to SiO_2 in the blended mix was high compared with GGBFS-CCA blended binders reported in this study. Therefore, it is inferred that RM

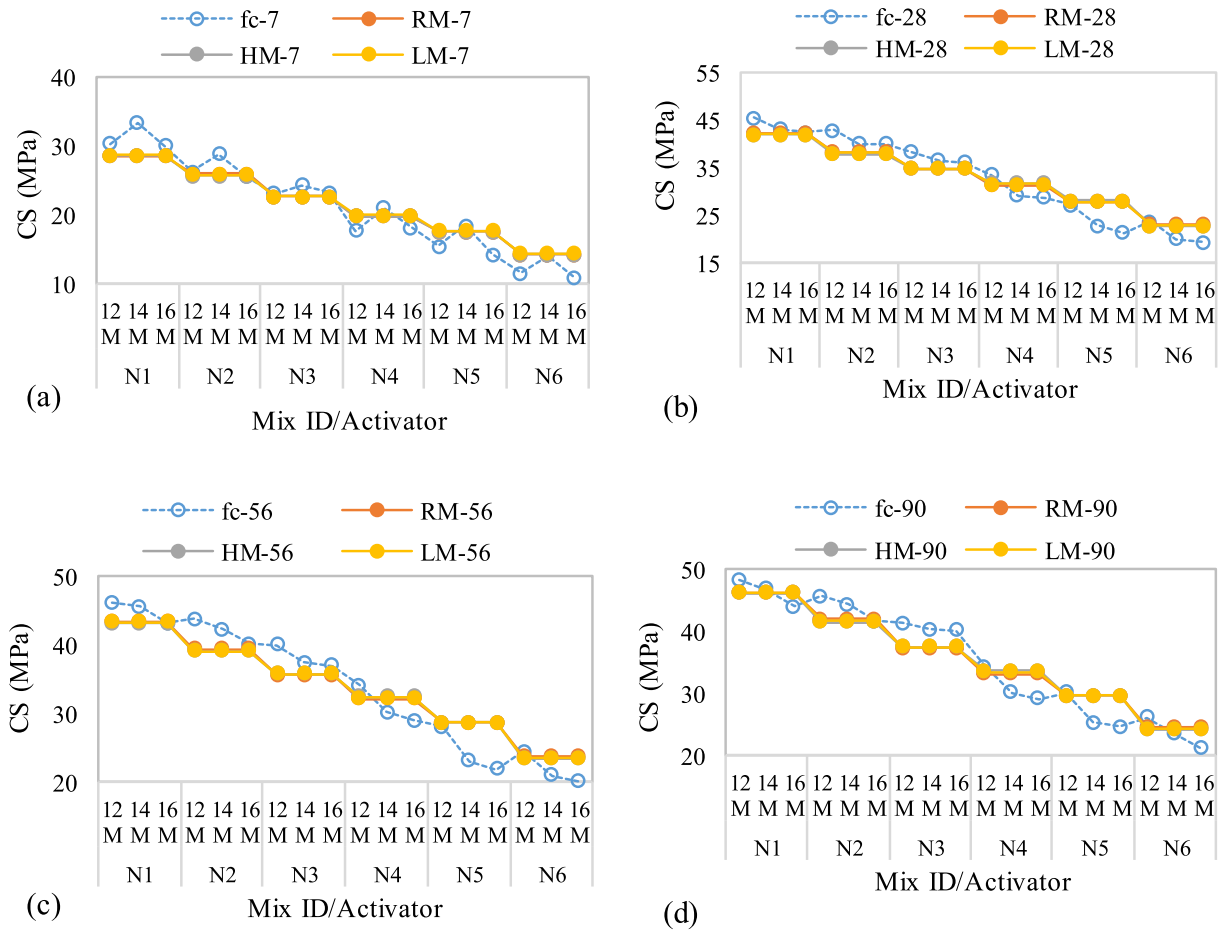

Fig. 12. Comparison of experimental results with predicted values for M 30 at (a) 7, (b) 28, (c) 56, and (d) 90 days curing.

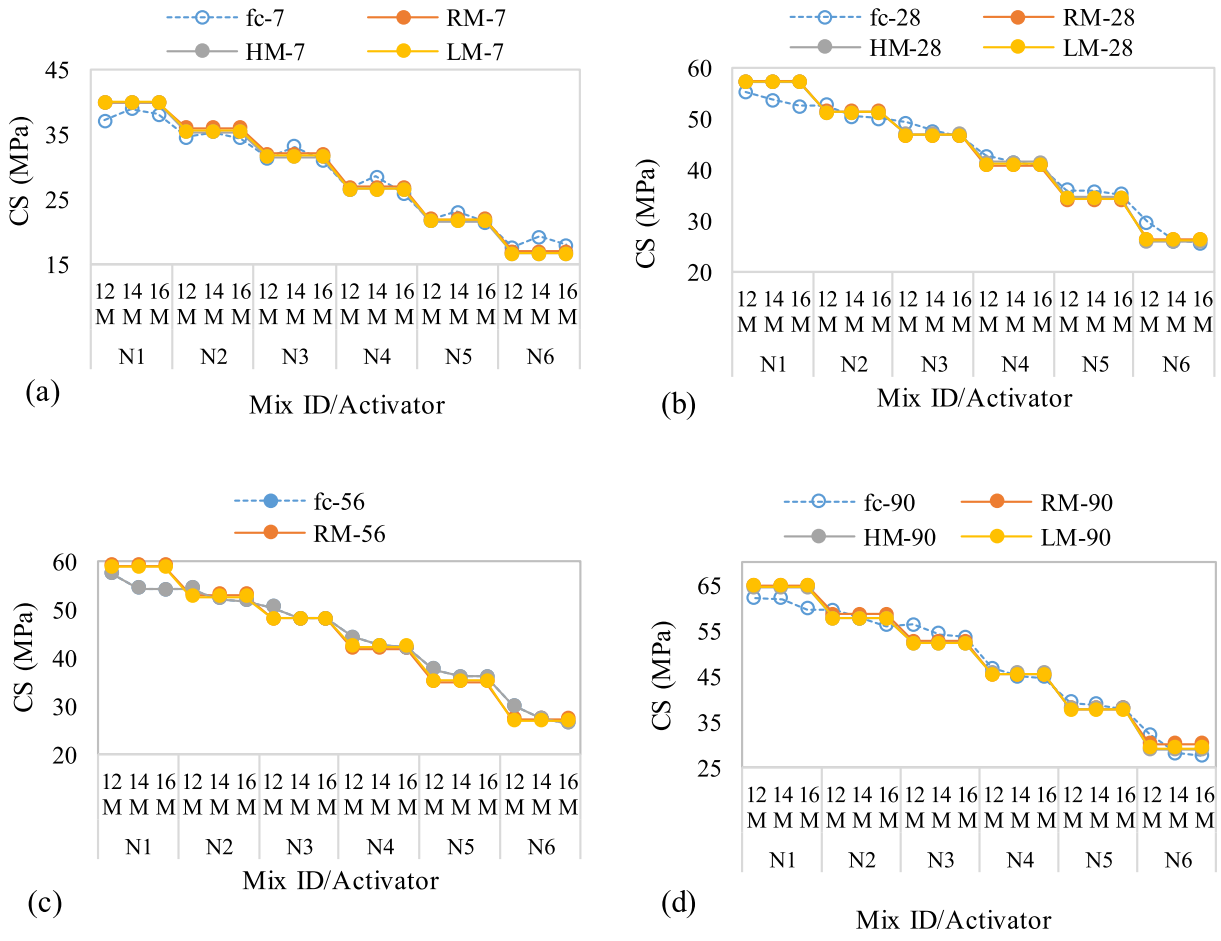

Fig. 13. Comparison of experimental results with predicted values for M 40 at (a) 7, (b) 28, (c) 56, and (d) 90 days curing.

yields the best fit for GGBFS-CCA blended binder, and this can be used in the validation of blended binders incorporating SCMs.

3.4.5. Validation of predictive models

Fig. 14 shows the validation of the predictive model based on the RIs (RM, AM, and SM), w/b ratio, and b/agg ratio with other similar predictive models at 28-day curing.

Fig. 14 indicates similar data points and trend lines for both experimental values and predictive values for both M 30 and M 40. However, both Xie and Visintin [10] and Oyebisi et al. [25]'s models deviated from both experimental and predictive data points. For Xie and Visintin [10]'s model, there was 41–70% decreased in strength as the percentage replacement of GGBFS by CCA increased from 20 to 100% compared with the predictive models for both M 30 and M 40. In the same vein, there was an average of 30 and 75% decreased in strength for Oyebisi et al. [25]' model as the percentage replacement of GGBFS by CCA increased from 20 to 100% compared with the predictive models for M 30 and M 40, respectively. The reason for these differences may be attributed to the diversity of oxide compositions of blended binders, type and chemical compositions of aggregates, mix design proportions, fineness, and specific surface area of the blended binders [10,36–42]. Besides, comparing the model data of this study such as GGBFS-CCA blended binder, w/b of 0.54 and 0.42, b/agg volume of 0.23 and 0.29, and target strengths of 30 MPa and 40 MPa with other models', Oyebisi et al. [25]'s model was only based on M 25 target strength of PC-CNSA blended binder with w/b and b/agg ratios as 0.618 and 0.194, respectively, hence contributing to the lowest predictive strength in Fig. 14 (b) compared with Fig. 14 (a). On the other hand, Xie and Visintin [10]'s model was based on the generated data of various SCMs (fly ash, SF, MK, BA, POFA, RHA, and VA) with ratios of w/b and b/agg volume as 0.25–0.90 and 0.045–0.359, respectively, and target strengths ranging from 0 to 120 MPa.

3.5. Chemical attacks

The presence of solid salts in a solution reacts with the hydrated cement paste and attacks the concrete. Ordinarily, solid salts do not attack concrete [36]. Fig. 15 (a) and (b) present the weight loss for both M 30 and M 40, respectively, while Fig. 16 (a) and (b) present the strength loss for both M 30 and M 40, respectively following the immersion of concrete samples in 5% $MgSO_4$ solution for 90 days. After 90 days of immersing concrete samples in sulfate solution, the effect of $MgSO_4$ solution was superior to that of Na_2SO_4 solution [90–92]; this justified the selection of $MgSO_4$ solution for this study. The weight loss in GPC samples, as shown in Fig. 15 (a) and (b) for both M 30 and M 40, ranged from 3 to 5% and 2–4%, respectively, compared with 15 and 14.32% weight loss in PCC after 90 days of exposure of concrete cubes in 5% $MgSO_4$ solution. On the other hand, the strength loss in GPC samples from Fig. 16 (a) and (b) varied from 7 to 10% and 6–8% against 17.98 and 16% in PCC samples for both M 30 and M40, respectively. These results confirm the findings reported in similar studies in that the weight loss and strength loss of GPC samples vary from 2 to 4% and 2–10%, respectively, compared with 10–20% and 15–29% weight loss and strength loss in PCC samples after 90 days of exposure in 5% $MgSO_4$, respectively [73,90–94]. However, Wallah and Rangan

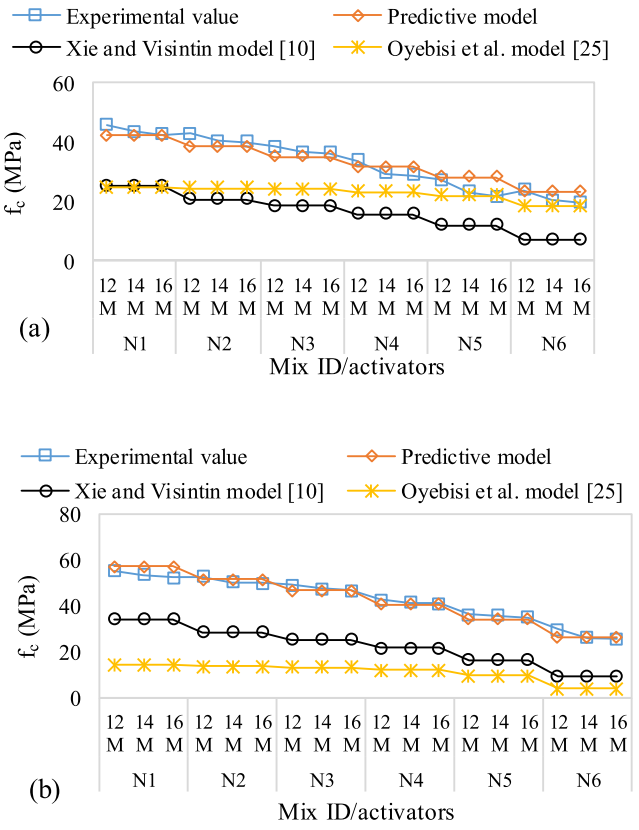

Fig. 14. Validation of developed models for (a) M 30 and (b) M 40.

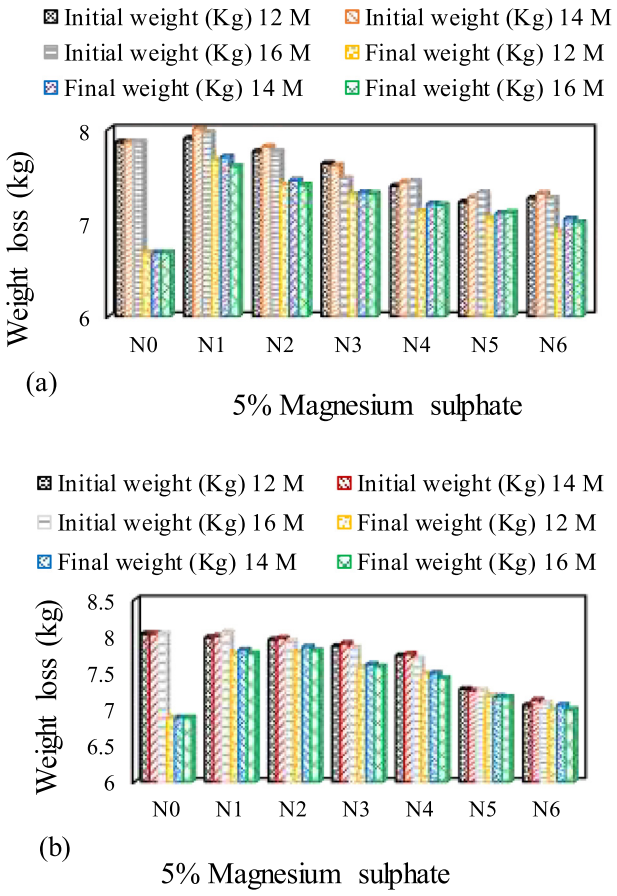

Fig. 15. Weight loss of cubes immersed in 5% $MgSO_4$ for (a) M 30 (b) M 40.

[92] and Hardjito et al. [93] also reported that a 5% $MgSO_4$ solution has no significant effect on the compressive strength and weight loss of GPC after 90 days of exposure. The PCC deterioration may be attributed to the critical consequence of magnesium sulfate attack on C-S-H, thus forming expansive gypsum and ettringite that induce expansion, spalling and cracking in the concrete [36,73]. In contrast to PCC, GPC, in general, do not have $Ca(OH)_2$ and mono-sulpho-aluminate in the matrix to cause expansion [36,74]. Therefore, it is inferred that GGBFS-CCA blended GPC resists more sulfate attack than PCC.

4. Conclusion

The study examined the GGBFS-CCA-based GPC, and its effects on the reactivity indexes and the sulfate attack were evaluated. Both experimental and statistical methods were used in the course of the study, and the results were compared with PCC. Consequent upon the findings and in line with research aims, the following sets of conclusions are made:

i. The reactivity of GGBFS-CCA blended binder increases with increasing CaO, MgO, and Al_2O_3 contents owing to the increase in GGBFS content, but the reactivity decreases with increasing SiO_2, Fe_2O_3, and SO_3 due to an increase in CCA content.
ii. The RM, HM, and LM of GGBFS-CCA blended binder increases with increasing CaO, MgO, and Al_2O_3 contents due to the GGBFS hydraulic response, while the SM and AM increase with increasing SiO_2 and Al_2O_3 contents owing to the CCA pozzolanic response.
iii. The RM, HM, LM, and AM of GGBFS-CCA blended binder increases by 10.6, 11.6, 11.6, and 3% with a 20% increase in GGBFS content, respectively, for both M 30 and M 40.
iv. The SM of GGBFS-CCA blended binder decreases by 6.8%, with a 20% increase in GGBFS content for both M 30 and M 40.
v. Compressive strength of GGBFS-CCA GPC increases with increasing RM, HM, LM, and AM.
vi. RM yields the best fit for predicting the compressive strength of slag-based GPC, incorporating CCA compared with HM and LM. Besides, a strong correlation exists between the experimental results and proposed model equations.
vii. There is no remarkable improvement in R^2 as the curing age increases.
viii. Slag-based GPC incorporating CCA provides good sulfate resistance superior to that of PCC.

The concept of RIs in predicting the compressive strength of the GGBFS-CCA blended mix is attainable, and the study affirms the efficiency of the fit regression model in Minitab 17 in predicting the compressive strength based on the RIs and the MDPs. This study benefits future research by focusing on three prospective solutions. First, the proposed model equations can be useful in the prediction and application of strength design proportions for GPC incorporating SCMs under ambient curing conditions provided the chemical compositions are obtained. Second, the application of SCMs, GGBFS and CCA, can be advantageous in high sulfate environment. Third, the recycling of both GGBFS and CCA would lessen the environmental, economic, and societal threats posed by the PC production; improve the concrete properties, and reduce the construction cost and solid wastes, hence driving sustainability.

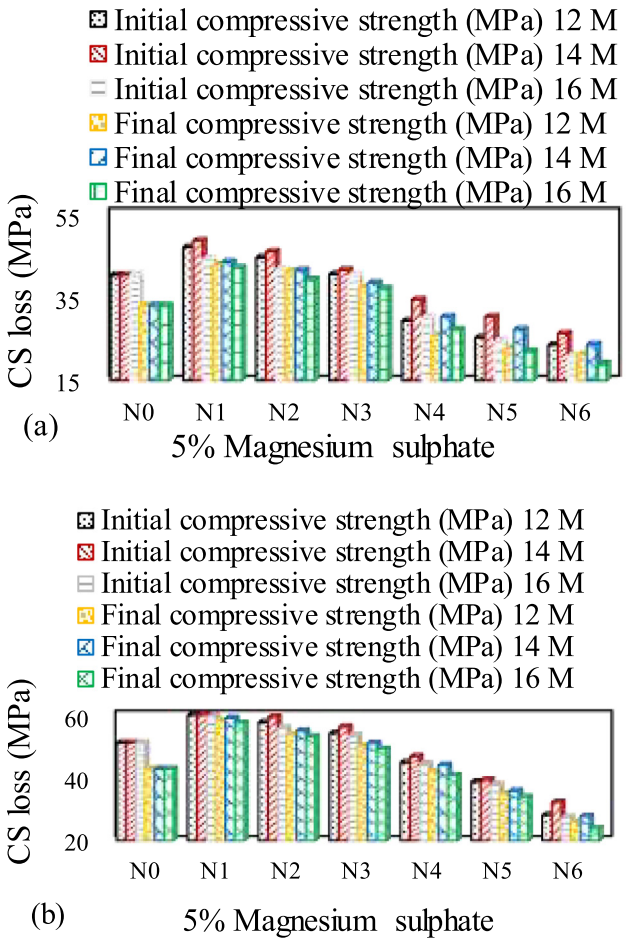

Fig. 16. CS loss of cubes immersed in 5% $MgSO_4$ for (a) M 30 (b) M 40.

CRediT authorship contribution statement

Solomon Oyebisi: Conceptualization, Data curation, Formal analysis, Funding acquisition, Investigation, Software, Methodology, Writing - original draft. **Anthony Ede:** Project administration, Resources, Supervision, Validation, Writing - review & editing. **Festus Olutoge:** Project administration, Resources, Supervision, Validation, Writing - review & editing. **Samuel Ogbiye:** Validation, Writing - review & editing.

Declaration of Competing Interest

The authors declare that they have no known competing financial interests or personal relationships that could have appeared to influence the work reported in this paper.

Acknowledgements

The researchers thank the Covenant University Centre for Research, Innovation, and Discovery (CUCRID) for the provision of the fund and conducive environment in carrying out the study.

References

[1] E.M. Fairbairn, B.B. Americano, G.C. Cordeiro, T.P. Paula, R.D. Toledo Filho, M.M. Silvoso, Cement replacement by sugar cane bagasse ash: CO_2 emissions reduction and potential for carbon credits, J. Environ. Manag. 91 (9) (2010) 1864–1871.
[2] L. Tosti, A. van Zomeren, J.R. Pels, R.N. Comans, Technical and environmental performance of lower carbon footprint cement mortars containing biomass fly ash as a secondary cementitious material, Res. Conserv. Recycl. 134 (2018) 25–33.
[3] C. Fan, S.A. Miller, Reducing greenhouse gas emissions for prescribed concrete compressive strength, Constr. Build. Mater. 167 (2018) 918–928.
[4] E. Crossin, The greenhouse gas implications of using ground granulated blast furnace slag as a cement substitute, J. Clean. Prod. 95 (2015) 101–108.
[5] P.J. Monteiro, S.A. Miller, A. Horvath, Toward sustainable concrete, Nat. Mater. 16 (7) (2017) 698.
[6] X. Bai, R.J. Dawson, D. Ürge-Vorsatz, G.C. Delgado, A.S. Barau, S. Dhakal, Six research priorities for cities and climate change, Nature 555 (7694) (2018) 23–25.
[7] E. Aprianti, P. Shafigh, S. Bahri, J.N. Farahani, Supplementary cementitious materials origin from agricultural wastes: a review, Constr. Build. Mater. 74 (2015) 176–187.
[8] G. Long, Y. Gao, Y. Xie, Designing more sustainable and greener self-compacting concrete, Constr. Build. Mater. 84 (2015) 301–306.
[9] S. Dadsetan, J. Bai, Mechanical and microstructural properties of self-compacting concrete blended with metakaolin, ground granulated blast furnace slag and fly ash, Constr. Build. Mater. 146 (2017) 658–667.
[10] T. Xie, P. Visintin, A unified approach for mix design of concrete containing supplementary cementitious materials based on reactivity moduli, J. Clean. Prod. 203 (2018) 68–82.
[11] S. Oyebisi, A. Ede, F. Olutoge, T. Igba, J. Ramonu, Rheology of slag-based geopolymer concrete using corncob ash as a pozzolanic material, IOP Conf. Series: Mater. Sci. Eng. 640 (2019), https://doi.org/10.1088/1757-899X/640/1/012057 012057.
[12] A.A. Raheem, S.O. Oyebisi, S.O. Akintayo, M.O. Oyeniran, Effects of admixture on the properties of corncob ash cement concrete, Leonardo Electron, J. Pract. Technol. 16 (2010) 13–20.
[13] A. Palomo, M.W. Grutzeck, M.T. Blanco, Alkali-activated fly ashes: a cement for the future, Cem. Concr. Res. 29 (8) (1999) 93–102.
[14] D.D. Adesanya, A.A. Raheem, Development of corn cob ash blended cement, Constr. Build. Mater. 23 (2009) 347–352.
[15] D. Khale, R. Chaudhary, Mechanism of geopolymerization and factors influencing its development: a review, J. Mater. Sci. 42 (2007) 729–749.
[16] D.A. Adesanya, A.A. Raheem, A study of the workability and compressive strength characteristics of corn cob ash blended cement concrete, Constr. Build. Mater. 23 (2009) 311–317.
[17] W. Chen, H. Brouwers, The hydration of slag, Part 1: reaction models for alkali-activated slag, J. Mater. Sci. 42 (2007) 428–443.
[18] F. Pacheco-Torgal, J. Castro-Gomes, S. Jalali, Alkali-activated binders: a review. Part 2, about materials and binders manufacture, Constr. Build. Mater. 22 (7) (2007) 1315–1322.
[19] S. Oyebisi, A. Ede, F. Olutoge, T. Igba, J. Oluwafemi, Effects of rest period on the strength performance of geopolymer concrete, IOP Conf. Series: Mater. Sci. Eng. 640 (2019), https://doi.org/10.1088/1757899X/640/1/012056 012056.
[20] A. Rajarajeswari, G. Dhinakaran, Compressive strength of GGBFS based GPC under thermal curing, Constr. Build. Mater. 126 (2016) 552–559.
[21] S. Oyebisi, J. Akinmusuru, A. Ede, O. Ofuyatan, G. Mark, J. Oluwafemi, 14 molar concentrations of alkaliactivated geopolymer concrete, IOP Conf. Series: Mat. Sci. Eng. 413 (2018), https://doi.org/10.1088/1757899X/413/1/012065 012065.
[22] S. Oyebisi, A. Ede, O. Ofuyatan, T. Alayande, G. Mark, J. Jolayemi, S. Ayegbo, Effects of 12 molar concentration of sodium hydroxide on the compressive strength of geopolymer concrete, IOP Conf. Series: Mat. Sci. Eng. 413 (2018), https://doi.org/10.1088/1757-899X/413/1/012066 012066.
[23] D.A. Adesanya, A.A. Raheem, A study of the permeability and acid attack of corn cob ash blended cements, Constr. Build. Mater. 24 (2010) 403–409.
[24] B. Lothenbach, K. Scrivener, R. Hooton, Supplementary cementitious materials, Cem. Concr. Res. 41 (12) (2011) 1244–1256.
[25] S. Oyebisi, T. Igba, D. Oniyide, Performance evaluation of cashew nutshell ash as a binder in concrete production, Case Stud. Constr. Mater. 11 (2019) e00293.
[26] S. Oyebisi, A. Ede, F. Olutoge, O. Ofuyatan, T. Alayande, Building a sustainable world: Economy index of geopolymer concrete, 10th Int. Struct. Eng. Constr. Conf. (ISEC-10), 2019. ISBN: 978-0-9960437-6-2.
[27] D. Saurabh, S. Yogesh, Comparison of geopolymer concrete based on strength and cost with concrete, Imperial, J. Interdiscipl. Res. 3 (9) (2017) 1026–1029.
[28] J. Thaarrini, S. Dhivya, Comparative study on the production cost of geopolymer and conventional concretes, Int. J. Civ. Eng. Res. 7 (2) (2016) 117–124.
[29] N. Dave, A.K. Misra, A. Srivastava, A.K. Sharma, S.K. Kaushik, Study on quaternary concrete microstructure, strength, durability considering the influence of multi-factors, Constr. Build. Mater. 139 (2017) 447–457.
[30] A. Darquennes, B. Espion, S. Staquet, Assessing the hydration of slag cement concretes, Constr. Build. Mater. 40 (2013) 1012–1020.
[31] T. Xie, T. Ozbakkaloglu, Influence of coal ash properties on compressive behaviour of FA-and BA- based GPC, Mag. Concr. Res. 67 (24) (2015) 1301–1314.
[32] E. Sakai, S. Miyahara, S. Ohsawa, S.H. Lee, M. Daimon, Hydration of fly ash cement, Cem. Concr. Res. 35 (6) (2005) 1135–1140.
[33] M. Behim, M. Beddar, P. Clastres, Reactivity of granulated blast furnace slag, Slovak J. Civ. Eng. 21 (2) (2013) 7–14.
[34] I. Alp, H. Deveci, Y.H. Sungun, A.O. Yilmaz, A. Kesimal, E. Yilmaz, Pozzolanic characteristics of natural raw material for use in blended cement, Iranian J. Sci. Technol. 33 (2009) 291–300.

[35] S. Wild, B. Sabir, J. Khatib, Factors influencing strength development of concrete containing silica fume, Cem. Concr. Res. 25 (7) (1995) 1567–1580.
[36] A.M. Neville, Properties of Concrete, Fifth ed., Pearson Education Ltd., England, 2011.
[37] V.G. Papadakis, S. Tsimas, Supplementary materials in concrete. Part I: Efficiency and design, Cem. Concr. Res. 32 (2002) 1035–1041.
[38] E. Rodriguez-Camacho, R. Uribe-Afif, Importance of using the natural pozzolans on concrete durability, Cem. Concr. Res. 32 (2002) 1851–1858.
[39] G. Habert, N. Choupay, J.M. Montel, D. Guillaume, G. Escadeillas, Effects of the secondary minerals of the natural pozzolans on their pozzolanic activity, Cem. Concr. Res. 38 (2008) 963–975.
[40] V.G. Papadakis, S. Antiohos, S. Tsimas, Supplementary materials in concrete. Part II: A fundamental estimation of the efficiency factor, Cem. Concr. Res. 32 (2002) 1533–1538.
[41] G.I. Obiefuna, P.H. Sini, A. Maunde, Geochemical and mineralogical composition of granitic rock deposits of Michika area North East, Nigeria, Int. J. Sci. Technol. Res. 7 (4) (2018) 160–170.
[42] A. Rittman, Using the Rittman serial index to define the alkalinity of igneous rocks, E Schwetzerbartsche Vealagsbuchandlung Stuttgart 184 (1) (1962) 95–103.
[43] E. Demoulian, P. Gourdin, F. Hawthorn, C. Vernet, Influence of Slags Chemical Composition and Texture on their Hydraulicity, Proceedings from Seventh International Conference on the Chemistry of Cement, Paris, FR, 2 (1980) 89-89.
[44] S. Donatello, M. Tyrer, C.R. Cheeseman, Comparison of test methods to assess pozzolanic activity, Cem. Concr. Compos. 32 (2010) 121–127.
[45] British Standard EN 15167-1, Ground Granulated Blast Furnace Slag for Use in Concrete, Mortar and Grout: Definitions, Specifications, and Conformity Criteria, BSI, London, 2006.
[46] American Society for Testing and Materials C 989, Standard Specification for Ground Granulated Blast-Furnace Slag for use in Concrete and Mortars, Annual Book of ASTM Standards: Philadelphia, PA, 2004.
[47] British Standard 3892-1, Pulverized-Fuel Ash: Specification for pulverized Fuel Ash for use with Portland Cement, BSI, London, 1997.
[48] British Standard EN 196-5, Methods of Testing Cement: Pozzolanicity Test for Pozzolanic Cement, BSI, London, 2011.
[49] American Society for Testing and Materials C-311, Standard Test Methods for Sampling and Testing Fly Ash or Natural Pozzolans for use in Portland-Cement Concrete, Annual Book of ASTM Standards: Philadelphia, PA, 2005.
[50] British Standard 7755-3, Soil Quality, Chemical Methods: Determination of pH, BSI, London, 1995.
[51] British Standard EN 1015-3, Methods of Test for Mortar for Masonry: Determination of Consistence of Fresh Mortar (by Flow Table), BSI, London, 1999.
[52] American Society for Testing and Materials C-618, Standard Specification for Coal Fly Ash and Raw or Calcined Natural Pozzolan for use in Concrete, Annual Book of ASTM Standards: Philadelphia, PA, 2005.
[53] American Society for Testing and Materials C1073-18, Standard Test Method for Hydraulic Activity of Slag Cement by Reaction with Alkali, ASTM International, West Conshohocken, PA, 2018.
[54] British Standard EN 196- 3, Method of testing cement: Physical Test. BSI, London, 2016.
[55] British Standard 1008, Mixing Water for Concrete: Specification for Sampling, Testing, and Assessing the Suitability of Water. BSI, London, 2002.
[56] N. P. Rajamane, R. Jeyalakshmi, Quantities of Sodium Hydroxide Solids and Water to Prepare Sodium Hydroxide Solution of Given Molarity for Geopolymer Concrete Mixes. Indian Concrete Institute Technical Paper, SRM University, India, 2014.
[57] P. Nath, P.K. Sarker, Effect of GGBFS on setting, workability and early strength properties of fly ash geopolymer concrete cured in ambient condition, Constr. Build. Mater. 66 (2014) 163–171.
[58] P. S. Deb, P. Nath, P. K. Sarker, Properties of Fly Ash and Slag Blended Geopolymer Concrete Cured at Ambient Temperature, New Dev. Struct. Eng. Constr. S. Yazdani, A. Singh, (Eds.) ISEC-7, Honolulu, June 18-23, 2013.
[59] N.P. Rajamane, M.C. Nataraja, R. Jeyalakshmi, Pozzolanic industrial waste-based geopolymer concretes with low carbon footprint, Indian Concr. J. 88 (7) (2014) 49–68.
[60] British Standard EN 12620, Aggregates from Natural Sources for Concrete, BSI, London, 2013.
[61] British Standard EN 450-1, Pozzolan for Use in Concrete: Definitions, Specifications, and Conformity Criteria, BSI, London, 2012.
[62] British Standard EN 8615-2, Specification for Pozzolanic Materials for Use with Portland Cement: High Reactivity Natural Calcined Pozzolana, BSI, London, 2019.
[63] N.M. Al Akhras, Durability of metakaolin concrete to sulfate attack, Cem. Concr. Res. 36 (9) (2006) 1727–1734.
[64] British Standard EN 196-2, Methods of Testing Cement: Chemical Analysis of Cement, BSI, London, 2016.
[65] British Standard EN 206, Concrete Specifications, Performance, Production and Conformity. BSI, London, 2016.
[66] British Standard 1881-125, Testing Concrete: Methods for Mixing and Sampling Fresh Concrete in the Laboratory, BSI, London, 2013.
[67] British Standard EN 12390-2, Testing Hardened Concrete: Making and Curing for Strength Tests, BSI, London, 2019.
[68] British Standard EN 12390- 4, Testing Hardened Concrete: Compressive Strength of Test Specimens, BSI, London, 2019.
[69] V. Sata, C. Jaturapitakkul, K. Kiattikomol, Influence of pozzolan from various by-product materials on mechanical properties of high-strength concrete, Constr. Build. Mater. 21 (7) (2007) 1589–1598.
[70] M.M. Johari, J. Brooks, S. Kabir, P. Rivard, Influence of supplementary cementitious materials on engineering properties of high strength concrete, Constr. Build. Mater. 25 (5) (2011) 2639–2648.
[71] S. Jamkar, C. Rao, Index of aggregate particle shape and texture of coarse aggregate as a parameter for concrete mix proportioning, Cem. Concr. Res. 34 (11) (2004) 2021–2027.
[72] N. Sebaibi, M. Benzerzour, Y. Sebaibi, N.E. Abriak, Composition of self-compacting concrete (SCC) using the compressible packing model, the Chinese method and the European standard, Constr. Build. Mater. 43 (2013) 382–388.
[73] B. Singh, G. Ishwarya, M. Gupta, S.K. Bhattacharyya, Geopolymer concrete: a review of some recent developments, Constr. Build. Mater. 85 (2015) 78–90.
[74] British Standard EN 16523-1, Determination of Material Resistance to Permeation by Chemicals, under the Conditions of Continuous Contact, BSI, London, 2015.
[75] I.I. Akinwumi, O.I. Aidomojie, Effect of corncob ash on the geotechnical properties of lateritic soil stabilized with Portland cement, Int. J. Geomat. Geosci. 5 (3) (2015) 375–392.
[76] H.F. Taylor, Cement Chemistry, London: Thomas Telford, 1997.
[77] P. Hewlett, Lea's Chemistry of Cement and Concrete, Third ed., p. 635-663, New York: John Wiley & Sons Inc., 2003.
[78] R.D. Hooton, Canadian use of ground granulated blast-furnace slag as supplementary cementing material for enhanced performance of concrete, Canadian J. Civ. Eng. 27 (4) (2000) 754–760.
[79] R.D. Hooton, J.J. Emery, Glass content determination and strength prediction for vitrified blast furnace slag. ACI SP-79 (2) (1983) 943-962.
[80] V. Dubovoy, Effects of Ground Granulated Blast-Furnace Slags on Some Properties of Pastes, Mortars and Concretes, Publication No. 897, Philadelphia: Blended Cement, ASTM, SP. Tech, 1986.
[81] J.C. Yang, Chemistry of Slag-Rich Cements: In Proceedings of the Fifth International Symposium on the Chemistry of Cement (Vol. 4, pp. 296-309), Tokyo, 1969.
[82] A. Gruskovnjak, B. Lothenbach, L. Holzer, R. Figi, F. Winnefeld, Hydration of alkali-activated slag: comparison with ordinary Portland cement, Adv. Cem. Res. 18 (3) (2006) 119–128.
[83] A. Gruskovnjak, B. Lothenbach, F. Winnefeld, B. Münch, R. Figi, S.C. Ko, U. Mäder, Quantification of hydration phases in super sulfated cement: review and new approaches, Adv. Cem. Res. 23 (6) (2011) 265–275.
[84] S. Pal, A. Mukherjee, S. Pathak, Investigation of hydraulic activity of ground granulated blast furnace slag in concrete, Cem. Concr. Res. 33 (9) (2003) 1481–1486.
[85] H.G. Smolczyk, Slag Structure and Identification of Slags, Proceedings from the 7th ICCC, 1: Cong. Chem. Cem. 1, Paris, 1-3, 1980.
[86] W. Matthes, A. Vollpracht, Y. Villagrán, S. Kamali-Bernard, D. Hooton, E. Gruyaert, M. Soutsos, N. De Belie, Ground Granulated Blast-furnace Slag. In: N. De Belie, M. Soutsos, E. Gruyaert, eds., Properties of Fresh and Hardened Concrete Containing Supplementary Cementitious Materials State-of-the-Art Report of the RILEM Technical Committee 238-SCM, Working Group 4, First ed. Springer International Publishing, 2018, pp. 2-46.
[87] A. Gruskovnjak, B. Lothenbach, F. Winnefeld, R. Figi, S.C. Ko, M. Adler, U. Mäder, Hydration mechanisms of super sulphated slag cement, Cem. Concr. Res. 38 (2008) 983–992.
[88] F. Winnefeld, M. Ben Haha, G. Le Saout, M. Costoya, S.C. Ko, B. Lothenbach, Influence of slag composition on the hydration of alkali-activated slags, J. Sust. Cem. Mater. 4 (2) (2015) 85–100.
[89] British Standard EN 197-1, Cement: Composition, Specifications and Conformity Criteria for Common Cements. British Standard Institution, 2 Park Street, London, 2016.
[90] V.M. Malhotra, M.H. Zhang, P.H. Read, J. Ryell, Long-term mechanical properties and durability characteristics of high-strength/high-performance concrete incorporating supplementary cementing materials under outdoor exposure conditions, Mate. J. 97 (5) (2000) 518–525.
[91] N.P. Rajamane, M.C. Nataraja, J.K. Dattatreya, N. Lakshamanan, D. Sabitha, Sulphate resistance and ecofriendliness of geopolymer concrete, The Indian Concr. J. 4 (2012) 13–22.
[92] S.E. Wallah, B.V. Rangan, Low Calcium Fly Ash based Geopolymer Concrete: Long Term Properties (pp. 0197), Research Report GC, Faculty of Engineering, Curtin University of Technology Perth, Australia, 2006.
[93] D. Hardjito, S.E. Wallah, D.M. Sumajouw, B.V. Rangan, Development of fly ash-based geopolymer concrete, ACI Mater. J. 101 (6) (2004) 55–64.
[94] S.H. Sanni, R. Khadiranaikar, Performance of geopolymer concrete under severe environmental conditions, Int. J. Civ. Struct. Eng. 3 (2) (2012) 396–407.